Sterol profiling of *Leishmania* parasites using a new HPLC-tandem mass spectrometry-based method and antifungal azoles as chemical probes reveals a key intermediate sterol that supports a branched ergosterol biosynthetic pathway

Mei Feng [a], Yiru Jin [a], Sihyung Yang [a], Arline M. Joachim [b], Yu Ning [c], Luis M. Mori-Quiroz [d], Jacob Fromm [a], Chamani Perera [d], Kai Zhang [c], Karl A. Werbovetz [b], Michael Zhuo Wang [a,*]

[a] *Department of Pharmaceutical Chemistry, School of Pharmacy, The University of Kansas, Lawrence, KS, USA*
[b] *Division of Medicinal Chemistry and Pharmacognosy, College of Pharmacy, The Ohio State University, Columbus, OH, USA*
[c] *Department of Biological Sciences, Texas Tech University, Lubbock, TX, 79409, USA*
[d] *Synthetic Chemical Biology Core Laboratory, The University of Kansas, Lawrence, KS, USA*

A B S T R A C T

Human leishmaniasis is an infectious disease caused by *Leishmania* protozoan parasites. Current chemotherapeutic options against the deadly disease have significant limitations. The ergosterol biosynthetic pathway has been identified as a drug target in *Leishmania*. However, remarkable differences in the efficacy of antifungal azoles that inhibit ergosterol biosynthesis have been reported for the treatment of leishmaniasis. To better understand the sterol biosynthetic pathway in *Leishmania* and elucidate the mechanism underlying the differential efficacy of antifungal azoles, we developed a new LC-MS/MS method to study sterol profiles in promastigotes of three *Leishmania* species, including two *L. donovani*, one *L. major* and one *L. tarentolae* strains. A combination of distinct precursor ion masses and LC retention times allowed for specific detection of sixteen intermediate sterols between lanosterol and ergosterol using the newly developed LC-MS/MS method. Although both posaconazole and fluconazole are known inhibitors of fungal lanosterol 14α-demethylase (CYP51), only posaconazole led to a substantial accumulation of lanosterol in azole-treated *L. donovani* promastigotes. Furthermore, a key intermediate sterol accumulated by 40- and 7-fold when these parasites were treated with posaconazole and fluconazole, respectively, which was determined as 4α,14α-dimethylzymosterol by high resolution mass spectrometry and NMR spectroscopy. The identification of 4α,14α-dimethylzymosterol supports a branched ergosterol biosynthetic pathway in *Leishmania*, where lanosterol C4- and C14-demethylation reactions occur in parallel rather than sequentially. Our results suggest that selective inhibition of leishmanial CYP51 is insufficient to effectively prevent parasite growth and dual inhibitors of both CYP51 and the unknown sterol C4-demethylase may be required for optimal antiparasitic effect.

1. Introduction

Leishmaniasis is an infectious disease caused by protozoan parasites in the genus *Leishmania* and is endemic in 97 countries and territories (World Health Organization, 2020). Depending on the causative species, leishmaniasis has two major clinical manifestations. Visceral leishmaniasis (VL), caused by *L. donovani* and *L. infantum*, shows infection of internal organs and is fatal if left untreated. Cutaneous leishmaniasis (CL), in which lesions develop at the site of sandfly bite, is caused by a variety of *Leishmania* species, e.g., *L. major* in the Old World and *L. mexicana* in the New World (Alemayehu and Alemayehu, 2017). It is estimated that 350 million people worldwide are at risk of infection (Dawit et al., 2013) with around 1.5 to 2 million new infections and 70,000 deaths each year (Torres-Guerrero et al., 2017; Seifert, 2011).

Leishmaniasis is the second most deadly parasitic disease after malaria (Oryan and Akbari, 2016).

To date, there is no prophylactic or therapeutic vaccine approved against human leishmaniasis (Ghorbani and Farhoudi, 2018; Palatnik-de-Sousa and Nico, 2020). Current chemotherapies for leishmaniasis are limited because of insufficient efficacy, serious adverse effects, emerging drug resistance, and/or high cost (Current Treatment of Leishmaniasis, 2174; Zulfiqar et al., 2017). Pentavalent antimonial drugs are the first-line therapies for all forms of leishmaniasis, but they show severe toxicities including cardiotoxicity, nephrotoxicity, pancreatitis, and hepatotoxicity, hence requiring additional clinical monitoring during intravenous injection (Oliveira et al., 2009; Wise et al., 2012). In North Bihar, India, failure of pentavalent antimonial drugs has been reported due to drug resistance in *L. donovani* (Sundar, 2001).

Paromomycin is an aminoglycoside antibiotic used for both CL and VL treatment and must be administered via the intramuscular route. The efficacy of paromomycin monotherapy varies between 36 and 96% based on the geographical location of the disease (Sundar et al., 2007; Hailu et al., 2010). Amphotericin B (AmB) is a macrolide polyene antifungal agent that binds to ergosterol in *Leishmania* membranes, increasing membrane permeability due to the formation of ion-channel pores and leading to cell death (Kumar et al., 2017; Gray et al., 2012). However, liposomal AmB (AmBisome®) is of high cost and requires hospitalization for slow intravenous infusion and a cold chain for storage and distribution (Freitas-Junior et al., 2012; de Menezes et al., 2015). Miltefosine is the only approved oral treatment for VL, but its use is limited by its high cost, gastrointestinal side effects, hepatotoxicity, nephrotoxicity, and notably, teratogenicity (de Menezes et al., 2015; Nagle et al., 2014). A decreasing miltefosine efficacy in Eastern Africa due to reduced exposure has been reported in recent years (Dorlo et al., 2017). Therefore, new safe and effective antileishmanial drugs with low cost are urgently needed.

The sterol biosynthetic pathway has been identified as a drug target in *Leishmania* because sterols are essential constituents of the *Leishmania* membranes for their normal structure and function (de Souza and Rodrigues, 2009). Like fungi, the main sterols of the *Leishmania* plasma membrane are ergosterol and ergosterol-like sterols rather than cholesterol in mammalian cells (de Souza and Rodrigues, 2009; Goad and Holz, 1984; McCall et al., 2015). Therefore, drugs that interfere with sterol biosynthesis have been evaluated for their antileishmanial activities. For example, terbinafine, a known squalene epoxidase inhibitor, exhibits promising antileishmanial activities (Urbina et al., 2002). Azasterols, which are inhibitors of the sterol 24-methyltransferase, show good *in vitro* activity against *Leishmania* parasites (Magaraci et al., 2003). Antifungal azoles, such as posaconazole (PSZ), fluconazole (FLU), ketoconazole (KTZ), itraconazole (ITCZ), clotrimazole, and ravuconazole, are known to interfere with ergosterol biosynthesis by inhibiting the lanosterol 14α-demethylase (CYP51) and they have been explored for their potential against leishmaniasis (Wali et al., 1990; Sousa et al., 2011; Teixeira de Macedo Silva et al., 2018; Joice et al., 2018; de Macedo-Silva et al., 2013). However, remarkable differences in the efficacy of antifungal azoles have been reported for the treatment of leishmaniasis. For example, KTZ was tested for four weeks in patients with VL and resulted in an 80% cure rate (Wali et al., 1990). On the other hand, ITCZ was tested for three months in patients afflicted with mucocutaneous leishmaniasis and only resulted in a 23% cure rate (Calvopina et al., 2004). It was reported that PSZ is approximately 12-times more potent than FLU against wild type *L. donovani* axenic amastigotes *in vitro* (Pandharkar et al., 2014) and that ITCZ is > 40-fold more potent than FLU and voriconazole against intracellular *L. major* amastigotes (Buckner and Wilson, 2005). Although it is uncertain what underlies the differing efficacies of antifungal azoles against *Leishmania*, their varying inhibitory activities against enzymes of *Leishmania* sterol biosynthesis may be a possible mechanism.

Gas chromatography-mass spectrometry (GC-MS) has been used for sterol and steroid analysis since the 1960s (Goad et al., 1997). Sterols can be analyzed by GC-MS either directly or in their chemically derivatized forms (Griffiths and Wang, 2009; Millerioux et al., 2018; Yao and Wilson, 2016). GC-MS has been widely applied as a reliable analytical method for the identification and quantification of sterols in *Leishmania* (Goad and Holz, 1984; Beach et al., 1979; Raederstorff and Rohmer, 1986). Sterol compositions of several *Leishmania* promastigotes have been identified and showed characteristics of yeast and other fungi (Goad and Holz, 1984). Promastigotes of six species of *Leishmania* were cultured in the presence of KTZ, ITCZ and FLU, and the effect of the different azoles on growth and sterol composition of each strain was evaluated. The inhibition by ITCZ was greater than or equal to KTZ, whereas FLU was the least active (Beach et al., 1988). Recently, high-performance liquid chromatography mass spectrometry (HPLC-MS) or LC-MS/MS has been applied for analysis of select sterols,

owing to a more straightforward identification and lack of requirement for derivatization steps (Nagy et al., 2006; Igarashi et al., 2011; Skubic et al., 2020; Trosken et al., 2004). However, no study has been reported for LC-MS/MS analysis of a complete panel of sterol intermediates between lanosterol and ergosterol. In this study, we developed an LC-MS/MS method to study the sterol profiles in promastigotes of three *Leishmania* species. We investigated the sterol profiles of *L. donovani* and *L. tarentolae* promastigotes with PSZ and FLU treatment. The intermediate sterol 4,14-dimethylzymosterol (4,14-DMZ) was purified from PSZ-treated *L. tarentolae* culture. And the stereochemistry of the C4 methyl group was assigned through two-dimensional (2D) heteronuclear multiple bond correlation (HMBC) and nuclear Overhauser effect (NOESY) NMR spectroscopy.

2. Materials and methods

2.1. Chemicals and reagents

Posaconazole (PSZ) was obtained from Carbosynth (Compton, UK). Fluconazole (FLU) was purchased from Cayman Chemical (Ann Arbor, MI). 5α-Cholesta-8,24-dien-3β-ol (zymosterol), 14-demethyl-14-dehydrolanosterol (FF-MAS), 4,4-dimethylcholesta-8,24-dien-3β-ol (T-MAS), cholesta-7,24-dienol, 7-dehydrodesmosterol, and cholesterol-d7 were purchased from Avanti Polar Lipids Inc. (Alabaster, AL). Ergosterol was acquired from Acros Organics (Geel, Belgium). M199 medium, squalene, hexane, and fetal bovine serum (FBS) were acquired from Sigma-Aldrich Corporation (St. Louis, MO). Lanosterol was obtained from American Radiolabeled Chemicals Inc. (St. Louis, MO). Episterol was purchased from Toronto Research Chemicals Inc. (North York, ON, Canada). Cholesterol was ordered from MP Biomedicals LLC (Irvine, CA). Optima LC/MS-grade water, optima-grade methanol, 2-propanol, formic acid, adenine, 10 N sodium hydroxide solution, and HEPES buffer (N-2-hydroxyethylpoperazine-N′-ethanesulfonic acid, pH 7.4) were bought from Fisher Scientific (Pittsburgh, PA). Hemin and DMSO were obtained from Alfa Aesar (Ward Hill, MA). Phosphate-buffer-saline (PBS) 10X was acquired from Mediatech Inc (Manassas, VA). Pen Strep and Schneider's Drosophila media were bought from Life Technologies Corporation (Grand Island, NY). Brain Heart Infusion (BHI) was purchased from Becton-Dickinson and Company (Sparks, MD).

2.2. Parasites and culture conditions

L. donovani 1S (Sudan) (Ld1s) strain and *L. major* LV39 clone 5 (Rho/SU/59/P) strain promastigotes were cultured at 27 °C in M199 medium (pH 7.4) with 10% heat-inactivated FBS and additional supplements (Kapler et al., 1990). Mid-log stage promastigotes ($4\text{-}7 \times 10^6$ cells/mL) were inoculated to 1×10^5 cells/mL and cultured to late log stage ($2\text{-}3 \times 10^7$ cells/mL). Promastigotes (1×10^8) from each strain were harvested by centrifugation and washed twice with PBS prior to sterol extraction as described below.

L. donovani LV82 (MHOM/ET/67:LV82) promastigotes were obtained by transformation of amastigotes collected from the spleen of an infected hamster. These parasites were cultured in Schneider's *Drosophila* medium containing 25% heat inactivated FBS, 50 U/mL penicillin, and 50 μg/mL streptomycin. LV82 parasite cultures were not used beyond sixteen passages as promastigotes. For the investigation of the sterol profile of LV82 promastigotes, parasite cultures were in late log phase ($\sim 10^8$ cells/mL) when they were used to prepare samples. To compare sterol profiles of *L. donovani* promastigotes treated with vehicle (0.4% [vol/vol] DMSO), PSZ (20 μM) and FLU (50 μM and 100 μM), LV82 promastigotes were seeded at 5×10^6 cells/mL in 25 cm² culture flasks. After 24 h incubation at 26 °C with an azole drug or the vehicle, parasites were counted using a hemocytometer, then 3×10^7 parasites were removed from each sample and centrifuged at 1800 *g* for 10 min at 4 °C. The supernatant was removed and the parasites were resuspended in 1.5 mL of cold PBS and aliquoted to 10^7 parasites/tube. Parasites were

centrifuged at 1800 *g* for 10 min at room temperature and the supernatant was removed. Cell pellets were stored at −80 °C until sterol extraction.

For the sterol profile study of drug-treated *L. tarentolae* promastigotes, *L. tarentolae* UC strain promastigotes were obtained from ATCC. Parasites were maintained as previously described (Yakovich et al., 2006). Briefly, the parasites were grown in autoclave-sterilized BHI medium (37 g/L supplemented with 10 mg/L filter-sterilized hemin, which was added from a 2 mg/mL stock dissolved in 0.05N NaOH, and 50 units/mL Pen/Strep, which was added from a 10,000 units/mL stock). Parasite cultures were in the late-log phase when they were used to prepare the samples described below, and they were not used beyond passage number fourteen. To compare sterol profiles of *L. tarentolae* promastigotes treated with vehicle (0.4% [vol/vol] DMSO), PSZ (5 μM) and FLU (40 μM), *L. tarentolae* promastigotes were seeded at 1×10^7 cells/mL in 250 mL flasks and maintained in an orbital shaker incubator (Thermo Scientific, Model 420) set at 125 rpm. After 24 h incubation at 26 °C with either an azole or the vehicle, parasites were counted using a hemocytometer, then washed twice with PBS buffer and stored at −80 °C until sterol extraction.

2.3. In vitro growth inhibition assay with L. donovani LV82 promastigotes

L. donovani promastigotes were added to 96 well plates and were incubated with serial two-fold dilutions of PSZ or FLU (200 nM–100 μM) or 0.5% DMSO vehicle (v/v) at cell density of 10^6 parasites/mL and a final volume of 100 μL in the medium described above. Plates were incubated for 72 h at 26 °C, then 20 μL of a 20:1 solution of 2 mg/mL 3-(4,5-dimethylthiazol-2-yl)-5-(3-carboxymethoxyphenyl)-2-(4-sulfo-phenyl)-2H-tetrazolium, inner salt (MTS):0.92 mg/mL phenazine methosulfate (PMS) in Dulbecco's Phosphate Buffered Saline was added to each well and the plate was incubated at 26 °C for 6–7 h. An additional 12 μL of a 10% SDS solution in distilled water was added to each well and the plate was incubated for an additional 1 h prior to measurement at 490 nm with a SpectraMax M5 microplate reader (Molecular Devices). Absorbance data were normalized with respect to the positive and negative control values. Average positive control absorbance values for each experiment were ≥2.5 and assays were considered valid if the calculated Z′ factor for the assay was ≥0.5.

2.4. In vitro growth inhibition assay with L. tarentolae

IC_{50} values of antifungal azoles (PSZ and FLU) on *L. tarentolae* promastigotes were determined with an assay adapted from the *L. donovani* axenic amastigotes IC_{50} assay (Delfin et al., 2009). Briefly, *L. tarentolae* promastigotes (2.5×10^5) were seeded in each well of a 96-well plate, then treated with different concentrations of PSZ (14 nM–30 μM) or FLU (27 nM–100 μM). Cells were incubated at 26 °C for 3 days in a water-jacketed incubator (Forma Scientific, Model 3546). Cell viabilities were determined using the MTT assay (Maarouf et al., 1997). The 96-well plates were centrifuged at 1500 *g* for 30 min at 4 °C and the supernatant was carefully removed. MTT reagent (50 μL; 2 mg/mL in PBS) was added to each well and the plates were incubated for an additional 3.5 h at 26 °C. After incubation, the plates were centrifuged at 1500 *g* for 30 min at 4 °C and the reagent was carefully aspirated. DMSO (100 μL) was added to dissolve the purple dye. The absorbance was measured at 540 nm using a plate reader (Tecan, Infinite M200 PRO).

2.5. Sterol extraction from Leishmania promastigotes

Free sterols were isolated using a hexane/isopropanol extraction method (Zhang et al., 2002) with modifications. Briefly, upon thawing on ice, parasite cell pellets (10^7 parasites for azole treatment studies and 10^8 parasites for sterol profile studies) were resuspended with 100 μL of cold PBS. After vortexing for 30 s, cold hexane-isopropanol (3:2 [vol/-vol]) extraction buffer (0.9 mL) containing an internal standard (IS; 50 nM cholesterol-d7) was added to the resuspended parasites and then vortex-mixed for another 30 s. After shaking at 1400 rpm (Eppendorf, Thermomixer R) for 15 min at 4 °C, samples were centrifuged at 14,000 rpm (Eppendorf centrifuge 5415C) for 5 min. The top layer (approximately 600 μL) was transferred to a clean 1.5 mL tube and dried under a stream of nitrogen at 50 °C using an evaporator (TurboVap LV, Zymark). The dried samples were reconstituted with 200 μL methanol prior to LC-MS/MS analysis.

2.6. Sterol analysis by LC-MS/MS

The analysis of sterols was performed using an LC-MS/MS system comprising a Waters Acquity I-Class UPLC with a binary pump, an FTN Sample Manager and a thermostatted column compartment, and a Xevo TQ-S triple quadrupole mass spectrometer (Waters Corporation). The ionization mode was electrospray chemical ionization (ESCI) positive ion mode: corona voltage, 2.5 kV; cone voltage, 30 V; source offset, 50 V; source temperature, 150 °C; desolvation temperature, 500 °C; desolvation gas flow, 1000 L/h; nebulizer gas, 7 bar. ESCI is equivalent to atmospheric pressure chemical ionization (APCI) and they are different only in that APCI is carried out in a dedicated ion source and ESCI is achieved using an electrospray ion source inserted with a corona discharge needle and operated under chemical ionization mode. Extracted sterols were separated on an Agilent ZORBAX Bonus-RP C18 column (2.1 mm × 150 mm, 5 μm) coupled with an Acquity column in-line filter (0.2 μm; Waters Corporation) equilibrated at 40 °C. LC mobile phases consisted of water containing 0.1% [v/v] formic acid (A) and methanol containing 0.1% [v/v] formic acid (B). The gradient started from 80% B and held for 3 min with a flow rate of 0.6 mL/min. Then, the mobile phase was increased from 80% B to 90% B over 12 min. After washing the column with 90% B for 4 min, the column was re-equilibrated with 80% B for 0.9 min before the next injection. The IS (cholesterol-d7) retention time was used to calibrate the retention times of other sterols monitored in the same LC injection. The total analysis time for each injection was 20 min. The injection volume was 10 μL. The characteristic multiple-reaction monitoring (MRM) transitions for sterols were listed in Table 1.

2.7. Purification of the proposed intermediate sterol 4,14-dimethylzymosterol from L. tarentolae promastigotes

L. tarentolae promastigotes were initially grown in the BHI medium described above in a 1L or 2L flask placed in an orbiting shaker incubator set at 125 rpm and 26 °C. Parasites were pelleted when reaching a density of 2–3 x 10^8 cells/mL by centrifugation (Eppendorf, centrifuge 5804R) at 1200 *g* at 4 °C. The parasites were subsequently resuspended in fresh BHI medium containing a final concentration of 5 μM PSZ (added from a 50 mM stock dissolved in DMSO) at a cell density of 2×10^8 cells/mL. After 24 h incubation, parasites were counted using a hemocytometer, then harvested by centrifugation at 1200 *g* at 4 °C. Cell pellets were washed twice with PBS and stored at −80 °C until sterol purification.

Free sterols were isolated using the modified hexane/isopropanol extraction described above. Briefly, upon thawing on ice, parasite cell pellets (6.3×10^{11} parasites) were resuspended with 10 mL of cold PBS. The resuspended parasites were sonicated with a handheld probe at power 10 (Fisher Scientific, Sonic Dismembrator Model 100) for 30 s. Cold hexane-isopropanol (3:2 [vol/vol]) extraction buffer (90 mL) was added to the parasites and then vortex-mixed for 15 min. Samples were centrifuged at 4500 *g* (Eppendorf, centrifuge 5804R) for 5 min at 4 °C. The top layer (60 mL) was transferred to a clean glass bottle. The extraction step was repeated two more times and the top layers were combined. The sterol extract was dried using a rotary evaporator at 50 °C and the dried extract was resuspended with DMSO/THF (1:1 v/v) prior to injection into a preparative LC-MS system for purification. Purification was carried out on a Waters Autopurification system

Table 1
LC-MS/MS detection of sterols and effects of posaconazole and fluconazole on the sterol levels in *Leishmania* parasites.

Sterol Group	Sterol Name	Molecular Weight (g/mol)	Retention Time (min)	Precursor Ion Mass (m/z)	Product Ion Mass (m/z)	Fold Change in Sterol Level[a]				
						L. donovani			*L. tarentolae*	
						PSZ[d] (20 μM) vs. Vehicle	FLU[d] (50 μM) vs. Vehicle	FLU (100 μM) vs. Vehicle	PSZ (5 μM) vs. Vehicle	FLU (40 μM) vs. Vehicle
4- and/or 14-methylated sterols	Lanosterol	426.7	13.5	409.3	109.1	21 ± 4***	1.0 ± 0.3	0.99 ± 0.33	11 ± 1***	2.0 ± 0.2***
	4,14-Dimethylzymosterol	412.7	12.5	395.4	135.1	40 ± 4.5***	7.1 ± 3.6*	6.5 ± 1.3**	16 ± 1***	8.7 ± 1.0***
	14-Methylzymosterol	398.7	11.1	381.4	109.1	1.1 ± 0.1	4.7 ± 1.2**	4.4 ± 2.0*	56 ± 15***	189 ± 53****
	14-Methylfecosterol	412.7	12.1	395.4	135.1	0.7 ± 0.3	89 ± 37*	90 ± 17***	5.1 ± 0.4***	4.9 ± 0.7****
	4-Methylzymosterol[b]	398.7	11.8	381.4	147.1	0.17 ± 0.12*	0.29 ± 0.11*	0.16 ± 0.04*	0[e]	1.1 ± 0.1
	FF-MAS	410.7	11.9	393.4	69.1	0.27 ± 0.08	0.30 ± 0.07	0.32 ± 0.12	ND[d]	ND
	T-MAS	412.7	13.2	395.4	135.1	0.31 ± 0.23*	0.33 ± 0.14*	0.17 ± 0.16**	ND	ND
4,14-demethylated sterols	Zymosterol	384.6	10.7	367.4	95.1	0.0 ± 0.0**	0.6 ± 0.3	0.36 ± 0.04*	0.07 ± 0.02***[c]	1.5 ± 0.2**[c]
	Fecosterol[b]	398.7	11.6	381.4	109.1	0.16 ± 0.12*	0.29 ± 0.10*	0.16 ± 0.04*	0[e]	1.1 ± 0.1
	Episterol[b]	398.7	11.8	381.4	147.1	0.16 ± 0.12*	0.29 ± 0.10*	0.11 ± 0.10*	0[e]	1.1 ± 0.1
	Cholesta-7,24-dienol	384.6	10.9	367.4	159.1	0.05 ± 0.05**	0.58 ± 0.28	0.28 ± 0.17*	0.07 ± 0.02***[c]	1.5 ± 0.2**[c]
5-dehydro sterols	7-Dehydrodesmosterol	382.6	10.0	365.4	159.1	0.07 ± 0.03*	0.08 ± 0.03*	0.05 ± 0.05*	0.03 ± 0.03***	0.81 ± 0.18
	5-Dehydroepisterol	396.7	10.9	379.2	145.0	0.56 ± 0.08	0.43 ± 0.11	0.33 ± 0.12*	<0.01	0.26 ± 0.04***
	Ergosta-5,7-dienol	398.7	12.7	381.4	147.1	0.31 ± 0.15	0.62 ± 0.40	0.56 ± 0.28	0[e]	0[e]
	Ergostatetraenol	394.6	9.7	377.3	109.1	0.23 ± 0.04	0.36 ± 0.10	0.33 ± 0.10	<0.01	0.39 ± 0.09**
	Ergosterol	396.7	11.6	379.2	145.0	0.31 ± 0.03	0.44 ± 0.13	0.38 ± 0.13	0.02 ± 0.01***	0.35 ± 0.04***

[a] mean ± standard deviation of triplicate determinations.
[b] Episterol, fecosterol and 4-methylzymosterol could not be chromatographically separated.
[c] Zymosterol and Cholesta-7,24-dienol could not be chromatographically separated.
[d] PSZ, posaconazole; FLU, fluconazole; ND, not detected in samples
[e] this sterol was detected in vehicle-treated, but not azole-treated samples.
*, **, *** unpaired two-tailed *t*-test (* P<0.05; ** P<0.01; *** P<0.001)

Color coding:
- fold≥32
- 32>fold≥8
- 8>fold≥2
- 2>fold≥0.5
- 0.5>fold≥1/8
- 1/8>fold≥1/32
- fold<1/32

with a Waters 2767 sample manager, a Waters 2525 HPLC pump, and a Waters 2996 photodiode array detector. LC mobile phases consisted of (A) water containing 0.05% [v/v] difluoroacetic acid and (B) acetonitrile containing 0.05% [v/v] difluoroacetic acid. A gradient elution was used for purification, which began from 80% to 100% B over 5 min and held at 100% B for 30 min with a flow rate of 20 mL/min. The sterols were separated on a Waters Atlantis T3 preparative C18 column (19 mm × 150 mm, 5 μm). The detection wavelength was set at 214 nm. For mass characterization, UPLC-HRMS analyses were carried out on a Waters Acquity UPLC with a photodiode array UV detector and an LCT Premiere TOF mass spectrometer. A Waters Acquity Atlantis T3 UPLC C18 column (2.1 mm × 50 mm, 1.7 μm) was used for separation and the column temperature was set at 35 °C. The detection wavelength was set at 214 nm. The gradient was from 80% to 95% B over 10 min and held at 95% B for 3 min with a flow rate of 0.6 mL/min.

2.8. NMR analysis of the proposed intermediate sterol 4,14-dimethylzymosterol

Around 10 mg of the purified sterol was dissolved in 0.6 mL of deuterated chloroform (CDCl$_3$). All NMR experiments (^{1}H, ^{13}C, DEPT, COSY, HSQC, HMBC, NOESY) were run on an Avance AVIII 500 MHz spectrometer equipped with a multinuclear BBFO cryoprobe. Chemical shifts (δ) are reported in ppm, and coupling constants are reported in Hz. The 7.26 ppm resonance of residual CHCl$_3$ for proton spectra and the 77.15 ppm resonance of CDCl$_3$ for carbon spectra were used as internal references. The known ^{1}H and ^{13}C NMR assignment of lanosterol was used as a reference for the structural assignment of the proposed intermediate sterol (Emmons et al., 1989).

2.9. Data analysis

Unless mentioned otherwise, all experiments were performed in triplicate. Student's *t* tests (unpaired, two-tailed) were used to compare the mean values of sterol levels in azole-treated parasites to that of vehicle control. One-way analysis of variance (ANOVA) followed by Tukey's test was used to evaluate sterol level differences between PSZ-treated, FLU-treated, and vehicle control parasites, where $P < 0.05$ was considered statistically significant. All data analyses were performed using GraphPad Prism (v. 9.3.1, San Diego, CA).

3. Results

3.1. MS/MS fragmentation of sterol standards and LC-MS/MS method development for sterol analysis

APCI (i.e., ESCI) was employed in this study to ionize sterols in the MS ion source, as sterol lipids are very hydrophobic and devoid of nitrogen-containing moieties. APCI was also the method of choice for LC/MS analysis of lanosterol and cholesterol oxides (Trosken et al., 2004). As expected, dehydrated molecular ions ([M+H–18]$^+$) were the predominant ions detected during MS full scan analysis before MS/MS fragmentation (data not shown) (Rossmann et al., 2007; Razzazi-Fazeli et al., 2000; Trosken et al., 2006). Upon collision-induced dissociation (CID), dehydrated molecular ions underwent extensive fragmentation as shown by the product ion scan spectra of sterol standards (Fig. S1). Major MS/MS fragments that were used for MRM method development in Table 1 are shown in Fig. 1 with proposed fragmentation pathways. The ion at 69.1 m/z was a common fragment that could be formed from the primary cleavage of the C22–C23 bond in the side chain of Δ^{24} sterols (double bond at C24–C25 position). In addition, many fragment ions were observed following secondary/tertiary fragmentation of the primary fragment ions that were formed after fragmentation at the C17–C20 bond. For example, the lanosterol primary fragment ion at 298.3 m/z further fragmented across the C-ring to produce fragment ions at 95.1, 109.1 and 123.1 m/z (Fig. 1). As a result, the 409.4 m/z precursor ion and 109.1 m/z product ion pair was chosen as the MRM transition for LC-MS/MS detection and quantification of lanosterol (Table 1). The lanosterol primary fragment ion at 298.3 m/z was observed at 297.4 and 299.5 m/z (Fig. S1A), presumably due to desaturation of the radical cation (298.3 m/z) in the MS collision cell to produce the 297.4 m/z ion and subsequent saturation of this ion to
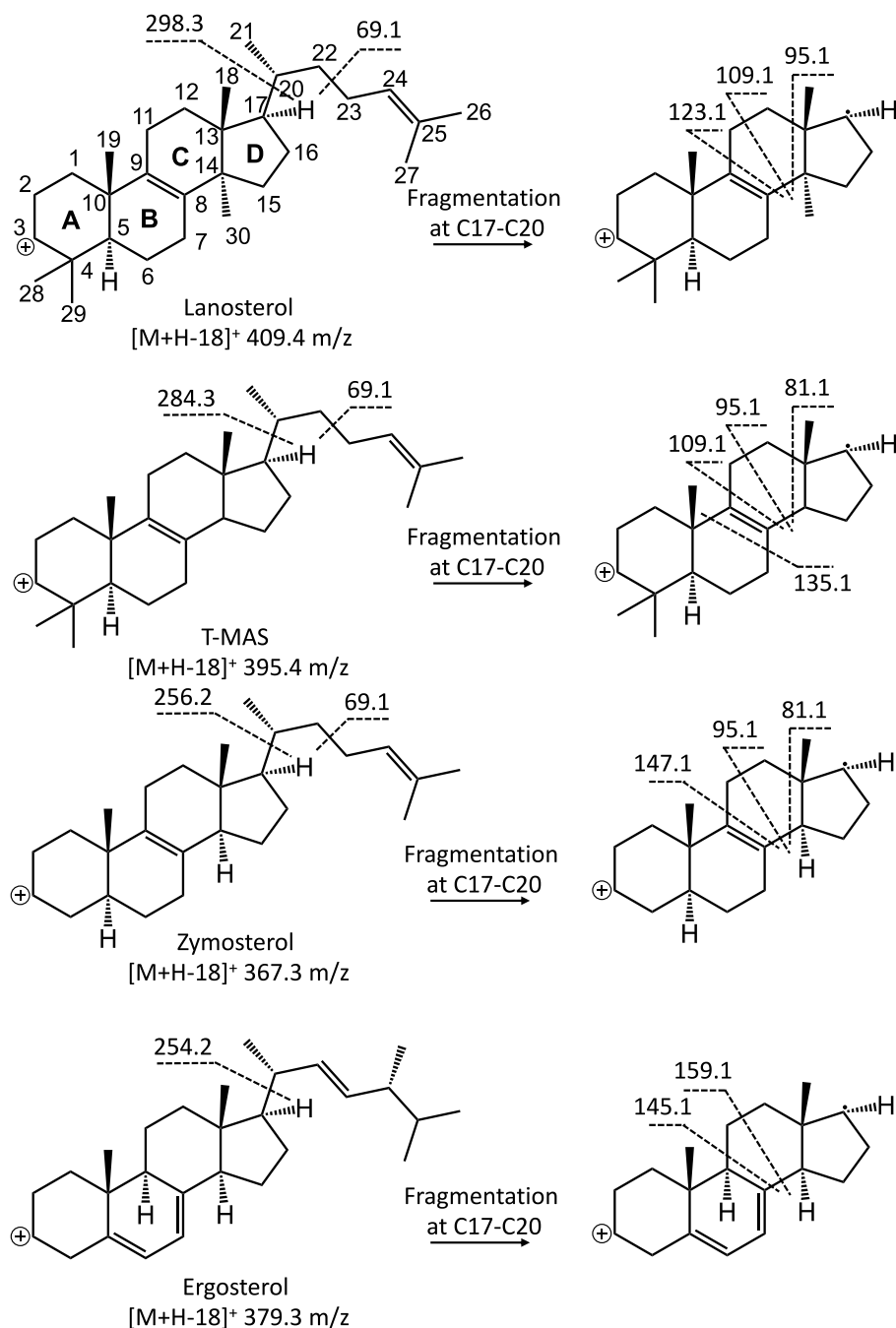
Fig. 1. Major MS/MS fragments of lanosterol, T-MAS, zymosterol and ergosterol and proposed CID fragmentation pathways.

produce the 299.5 m/z ion. In comparison to lanosterol, T-MAS (a 14-desmethylated sterol) produced a different set of fragment ions (81.1, 95.1 and 109.1 m/z) upon fragmentation across the C-ring with a mass shift of 14 Da due to the removal of the C30 methyl at the C14 position (Fig. 1). This pattern of 14 Da mass shift could be observed for other sterols and resulted in product ions with degenerate masses (Fig. S1). This has made it difficult to use distinctive fragment ions for specific MS/MS detection of sterols. As a result, product ions for MRM method development were chosen for their intensity rather than specificity for each individual sterol and a good LC separation was hence required for specific detection of sterols having the same molecular weight.

To achieve a good LC separation of sterols, it was reported that a relatively hydrophilic reversed phase column (e.g., Aquasil C18) provided more retention and selectivity for the separation of cholesterol

oxides (Razzazi-Fazeli et al., 2000). Another study employed a reversed phase C8 column (e.g., Symmetry Shield C8) to separate lanosterol and FF-MAS (Trosken et al., 2004). In our study, reversed phase Zorbax Bonus-RP columns provided good separation and efficient elution of sterol standards, resulting in optimal peak shape and very little peak tailing (Fig. 2A). The unique characteristics of Zorbax Bonus-RP stationary phase chemistry may have contributed to the desirable results. For example, the embedded polar amide group is designed to reduce unwanted silanol interactions and enable earlier elution of highly hydrophobic molecules at a lower concentration of organic mobile phase than what's required for a traditional long-chain alkyl stationary phase (e.g., C18 or C8). When Aquasil C18 or Symmetry Shield C8 columns were used, elution was achieved using isocratic 60/40 acetonitrile/methanol or 98% methanol for cholesterol oxides and lanosterol/FF-MAS, respectively (Trosken et al., 2004; Razzazi-Fazeli
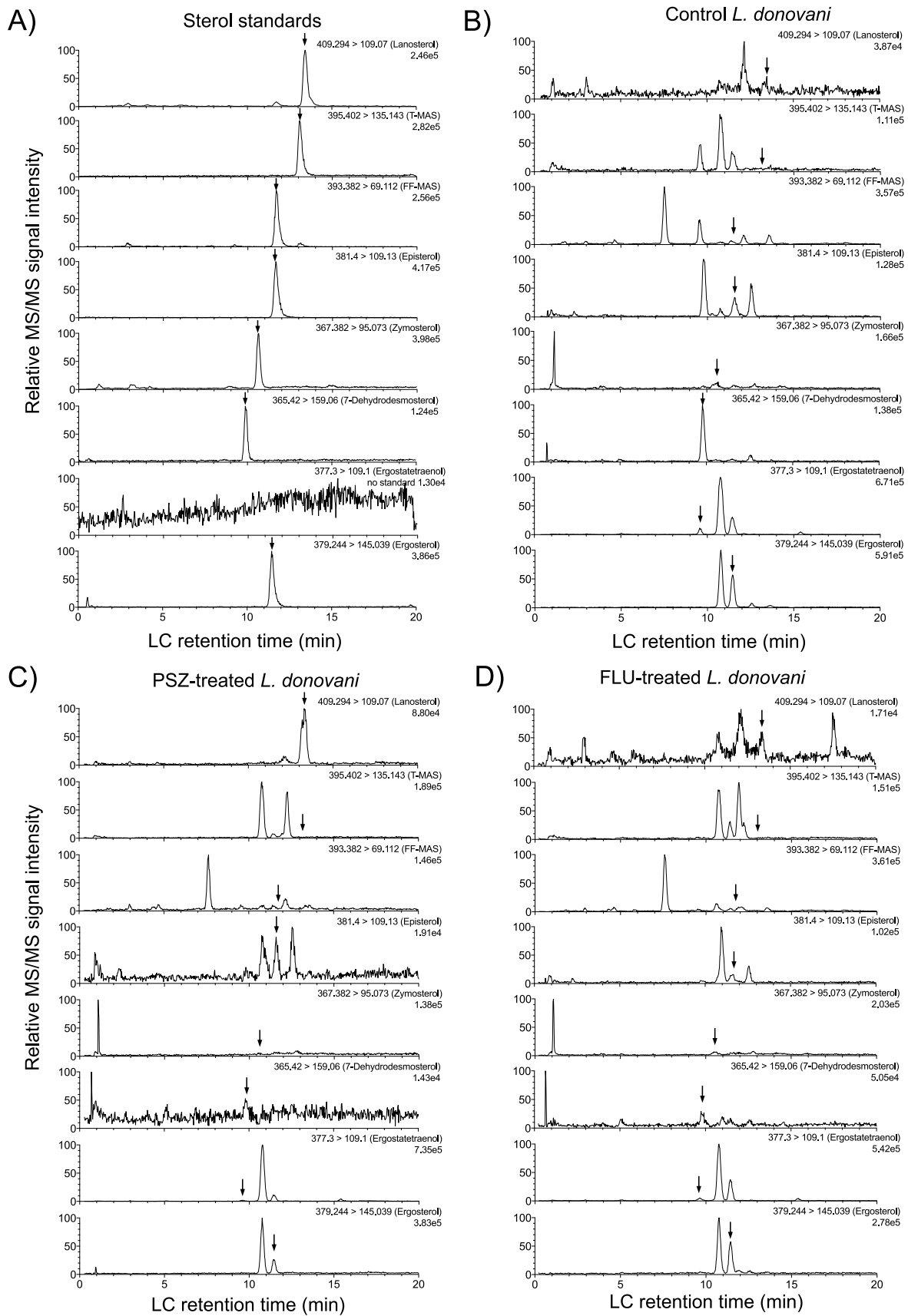
Fig. 2. Representative LC-MS/MS chromatograms of sterol standards (A) and extracted sterols from *Leishmania donovani* LV82 promastigote parasites treated with the vehicle (B), posaconazole (C), or fluconazole (D). Corresponding MRM transitions and retention times can be found in Table 1. LV82 promastigotes were treated with 0.4% DMSO vehicle, 20 μM PSZ, or 50 μM FLU. Arrows indicate the LC retention time of corresponding sterol standards.

et al., 2000). In contrast, gradient elution of seven sterol standards was achieved between 80 and 90% methanol over 12 min using a Zorbax Bonus-RP column (Fig. 2A). Importantly, sterol LC retention time was stable through multiple LC injections. For example, the IS (cholesterol-d7) retention time averaged (± standard deviation) 12.72 ± 0.08 min (0.6% CV) and 12.44 ± 0.03 min (0.3% CV) for the twelve consecutive injections in Fig. 3 and another twelve consecutive injections in Fig. 4, respectively. Overall, our new method requires only 20 min of LC analysis time (including gradient separation and column re-equilibration) for each sample injection.

More importantly, the combination of distinct precursor ion masses and different LC retention times allowed for specific detection of each sterol standard using the newly developed LC-MS/MS method (Table 1). In addition, it was observed that reversed phase LC retention times reflect structural differences of the sterols. Sterols with additional methyl/methylene groups and/or saturated carbon-carbon bonds eluted later than those without. For example, lanosterol (13.5 min) has one additional methyl group at the C-14 position than T-MAS (13.2 min) and T-MAS has one additional saturated C14–C15 bond than FF-MAS (11.9 min). Similarly, episterol (11.8 min) and ergosterol (11.6 min) have one additional methylene group at the C-24 position than zymosterol (10.7 min) and 7-dehydrodesmosterol (10.0 min), respectively; and cholesta-7,24-dienol (10.9 min) has one addition saturated C5–C6 bond compared to 7-dehydrodesmosterol (10.0 min). This relationship between LC retention time and sterol structure was used to postulate structures of additional sterols present in the *Leishmania* parasites when authentic standards were not available, e.g., 4,14-dimethylzymosterol, 14-methylzymosterol, 14-methylfecosterol, 4-methylzymosterol, fecosterol, 5-dehydroepistrerol, ergosta-5,7-dienol and ergostatetraenol

(Table 1 and Scheme 1). Because episterol, fecosterol and 4-methylzymosterol have the same molecular weight and precursor ion mass (m/z 381.4) and they eluted very closely to each other (11.8, 11.6 and 11.8 min), our LC-MS/MS method was not able to resolve these sterols; therefore the episterol quantification reported herein comprises all three sterols. Similarly, zymosterol (10.7 min) and cholesta-7,24-dienol (10.9 min) could not be fully resolved chromatographically, but separate peaks could be integrated on the partially separated sterols for their quantification.

3.2. Comparison of sterol profiles between L. donovani, L. major, and L. tarentolae promastigotes

Free sterols (unesterified) have been shown to reflect the effect of antifungal azoles on *Leishmania* (Beach et al., 1988) and the impact of genetic deletion of sterol biosynthetic enzymes in *Leishmania* (Xu et al., 2014). As such, profiles of free sterols of *L. donovani* (strains LV82 and Ld1s), *L. major* (strain LV39), and *L. tarentolae* (strain UC) were determined using the new LC-MS/MS method. The IS-normalized LC-MS/MS peak areas of thirteen sterols from these *Leishmania* promastigotes cultured *in vitro* are shown in Fig. 3. Many intermediate sterols between lanosterol and ergosterol from the canonical linear sterol biosynthetic pathway (Scheme 1) could be identified in all three *Leishmania* species. These included lanosterol, 14-methylzymosterol, zymosterol, episterol/fecosterol/4-methylzymosterol, 5-dehydroepisterol, ergostateraenol, and ergosterol. Unexpectedly, FF-MAS was not detected in any of the *Leishmania* promastigotes and a low level of T-MAS was detected in the promastigotes of two *L. donovani* strains. Furthermore, several intermediate sterols belonging to the proposed branched sterol
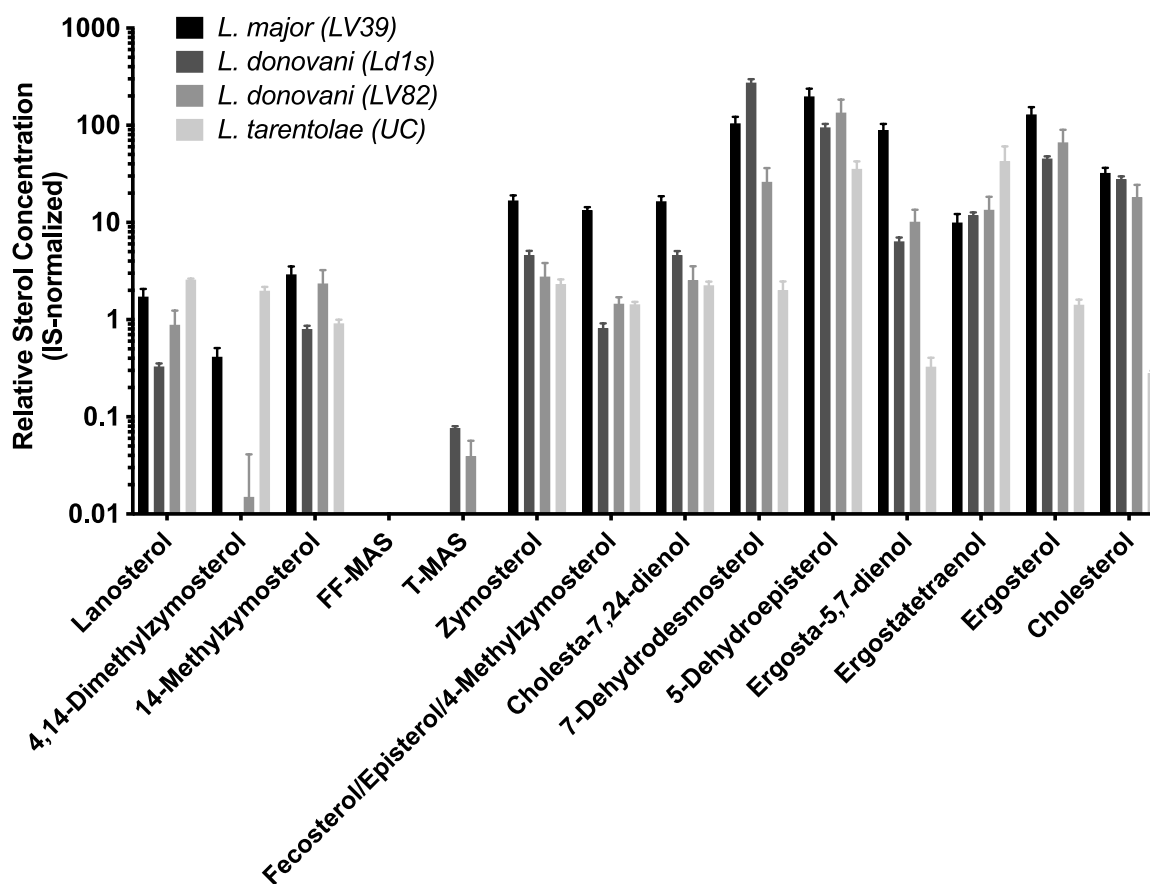

Fig. 3. Comparison of sterol profiles for *Leishmania* promastigotes of different species. Relative quantification of each sterol among different species was achieved by extracting free sterols from 10^8 parasites and normalizing LC-MS/MS signals by internal standard spiked into each sample. Bars and error bars represent the mean and standard deviation of triplicate determinations.
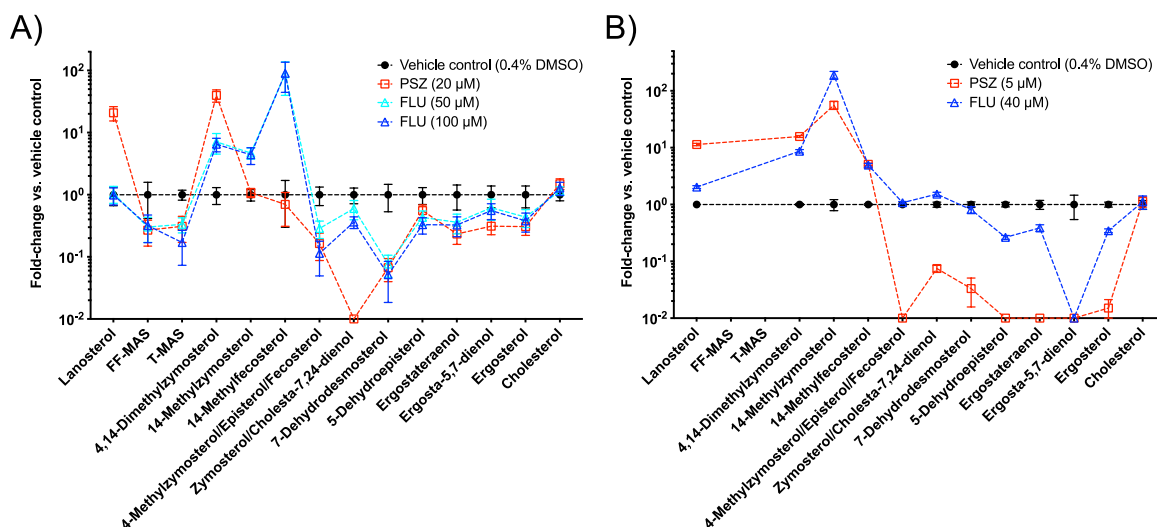
Fig. 4. Differential effects of posaconazole (squares) and fluconazole (triangles) on the sterol profiles of *L. donovani* (A) *and L. tarentolae* (B) promastigotes. Fold change vs. vehicle control was calculated by taking the ratio of IS-normalized LC-MS/MS signals of each sterol between antifungal azole-treated and vehicle-treated promastigotes. Bars and error bars represent the mean and standard error of three independent measurements. The lines connecting the symbols are to distinguish different treatments and the order of sterols on the x-axis is arranged to follow the conversion of 4- and/or 14-methylated sterols to 4,14-demethylated sterols, then to 5-dehydro sterols from left to right as shown in the Scheme 1.
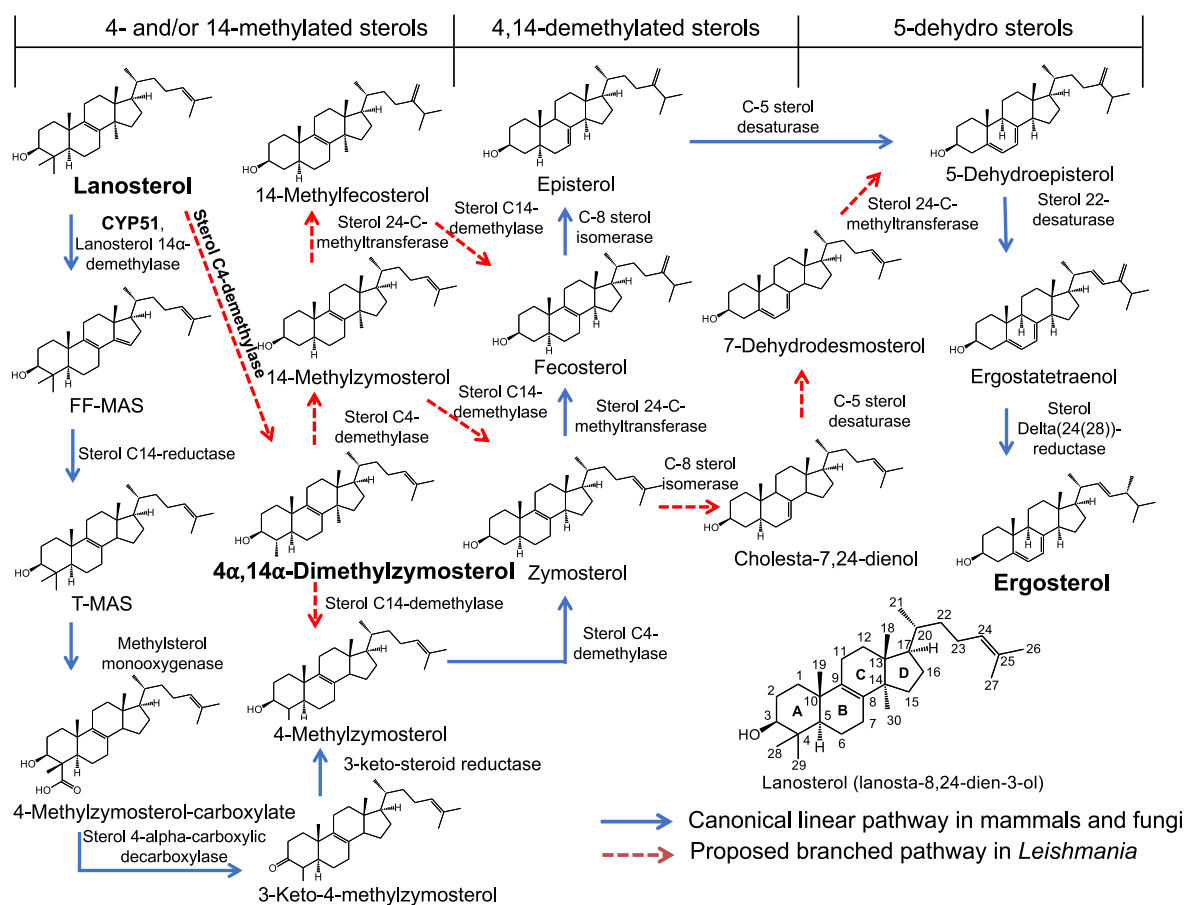
Scheme 1. Proposed branched ergosterol biosynthesis pathway in *Leishmania*. A similar pathway was proposed previously by Goad et al. (Goad and Holz, 1985).

biosynthetic pathway (Scheme 1) were detected in the three *Leishmania* species. These included 4,14-dimethylzymosterol, 14-methyl-zymosterol, cholesta-7,24-dienol, and 7-dehydrodesmosterol, although 4,14-dimethylzymosterol was below the limit of detection in one (Ld1s)

of the two *L. donovani* strains.

3.3. Differential effects of posaconazole and fluconazole on the sterol profile of Leishmania promastigotes

Consistent with previous studies examining the effects of PSZ and FLU on *Leishmania* (de Macedo-Silva et al., 2013; Pandharkar et al., 2014; Buckner and Wilson, 2005), PSZ inhibited *L. donovani* promastigote growth at micromolar concentrations over a period of 72 h, while FLU exhibited a much weaker effect on *L. donovani* proliferation (Fig. S2). Similarly, PSZ was a much stronger inhibitor of *L. tarentolae* promastigote growth than FLU over a range of concentrations (Fig. S3). Sterol profiles of *L. donovani* and *L. tarentolae* promastigotes incubated with or without these antifungal azoles are shown in Fig. 4 and Table 1. As expected, antifungal azole treatments reduced the level of many intermediate sterols in the promastigotes relative to the vehicle-treated promastigotes. These included 5-dehydro sterols (ergosterol, ergostatetraenol, 5-dehydroepisterol, ergosta-5,7-dienol, and 7-dehydrodesmosterol) and 4,14-demethylated sterols (zymosterol, fecosterol, episterol, and cholesta-7,24-dienol). In addition, low levels of FF-MAS and T-MAS were detected in the untreated *L. donovani* LV82 promastigotes and were further reduced upon antifungal azole treatments, likely due to inhibition of the leishmanial CYP51 by antifungal azoles, leading to the decreased production of these 14-demethylated metabolites of lanosterol (Scheme 1). Neither FF-MAS nor T-MAS was detectable in the *L. tarentolae* promastigotes before or after antifungal azole treatments. It should also be noted that there was not a significant change in the cholesterol level after antifungal azole treatment (Fig. 4). This is consistent with the result reported by Xu et al. where the *CYP51* gene was deleted from *L. major*, (Xu et al., 2014) although an earlier report by Beach et al. showed a greater change in the cholesterol level after antifungal azole treatment (Beach et al., 1988).

Interestingly, several intermediate sterols from the proposed branched sterol biosynthetic pathway (Scheme 1) saw substantial accumulation upon antifungal azole treatments and the pattern of accumulation showed a clear difference between the PSZ and FLU treatments. For example, in the *L. donovani* promastigotes, lanosterol, a known substrate of CYP51, accumulated when treated with PSZ (21-fold), but not FLU (1-fold) (Table 1). 4,14-Dimethylzymosterol accumulated by 40-fold and, to a lesser degree, 7-fold when treated with PSZ and FLU, respectively. In contrast, 14-methylfecosterol increased by about 90-fold when treated with FLU, whereas no accumulation was observed when treated with PSZ (Table 1). In the *L. tarentolae* promastigotes, lanosterol accumulated by 11-fold and, to a much less degree, 2-fold when treated with PSZ and FLU, respectively (Table 1). 4,14-Dimethylzymosterol accumulated by 16-fold and 8.7-fold when treated with PSZ and FLU, respectively. Instead of 14-methylfecosterol, 14-methylzymosterol (a 24-C desmethylated analog of 14-methylfecosterol; Scheme 1) showed the greatest accumulation by 56-fold and 189-fold when treated with PSZ and FLU, respectively. Taken together, posaconazole and fluconazole exerted different effects on sterol profiles of *Leishmania* promastigote parasites and a proposed novel intermediate sterol, 4,14-dimethylzymosterol, was highly accumulated in antifungal azole-treated parasites.

3.4. Purification and structural determination of an unknown intermediate sterol 4,14-dimethylzymosterol that is key to the proposed branched ergosterol biosynthesis pathway in Leishmania

Due to the similar sterol profiles and effects of antifungal azole treatments as shown above and the ease of culturing non-pathogenic organisms at high cell densities, *L. tarentolae* promastigotes were selected as a surrogate system to *L. donovani* to biosynthesize the key intermediate sterol, 4,14-dimethylzymosterol, for HPLC purification and structural elucidation using NMR. Two liters of *L. tarentolae* culture with a final concentration of 5 μM PSZ yielded 6.3×10^{11} parasites after 24 h incubation. After sterol extraction and purification by preparative chromatography, approximately 4.3 mg of the target sterol with greater than 99% purity was obtained. The predicted exact mass of 4,14-dimethylzymosterol was 412.37 Da and it was expected to produce a dehydrated ($[M+H–18]^+$) precursor ion mass of 395.37 m/z, which was confirmed by the high resolution TOF mass spectrometry (Fig. 5A).

The 1D and 2D NMR spectra of a lanosterol standard and the unknown sterol were obtained and shown in Fig. 5B to I and Figs. S4–S6. The data analysis focused on the chemical shifts of the methyl groups in lanosterol and in the unknown, as well as their 2D correlations with neighboring proton and carbon atoms. The absolute structure of the unknown target sterol was resolved as 4α,14α-dimethylzymosterol, which lacks "methyl 29" with respect to lanosterol. The 1D ^{1}H and ^{13}C NMR spectra of the compound were consistent with data presented earlier for 4,14-dimethylzymosterol (4α,14α-dimethylcholesta-8,24-dien-3β-ol) (Goad and Holz, 1985). Key observations included: (i) 7 methyl groups in the unknown, whereas 8 methyl groups were present in lanosterol (Fig. 5B and C); (ii) 3 quaternary carbon atoms in the unknown (Fig. 5E), whereas 4 quaternary carbon atoms were present in lanosterol (Fig. 5D); (iii) C28 protons present as a doublet in the unknown, whereas C28 and C29 protons occurred as singlets in lanosterol (Fig. 5B); (iv) HMBC correlations of C28 protons with neighboring carbon atoms C3, C4, and C5, similar to the correlations of C19 protons with neighboring carbon atoms C5 and C10 (indicated by blue arrows in Fig. 5G); (v) NOESY correlations between H3/H5 and H3/H28 (Fig. 5I).

4. Discussion

Although the intermediate sterol 4α,14α-dimethylzymosterol has been isolated from ketoconazole-treated *L. mexicana* promastigotes and identified by GC-MS using relative retention times and MS fragments and by ^{1}H NMR and ^{13}C NMR in 1980s (Goad and Holz, 1985; Berman et al., 1984), the stereochemistry of the C4 and C14 methyl groups was only tentatively assigned. In the present study, we were able to elucidate the stereochemistry of 4α,14α-dimethylzymosterol at C4 using 2D NMR. Instead of purifying this sterol from *L. donovani* or *L. mexicana*, *L. tarentolae* was cultured for sterol purification for the following three reasons. First, a higher cell density ($>2.6 \times 10^8$ cells/mL) can be achieved in *L. tarentolae* culture using a relatively inexpensive medium (Fritsche et al., 2007). Second, *L. tarentolae* was easier to handle in larger scale culture since it's non-pathogenic to humans. Third, *L. tarentolae* shares >90% of its genes with other pathogenic *Leishmania* species, including *L. donovani* and *L. mexicana* (Raymond et al., 2012), and similar changes in sterol profiles were observed after antifungal azole treatment as shown in this study.

The newly developed LC-MS/MS sterol analysis method will allow a more comprehensive analysis of the key intermediates involved in the sterol biosynthesis pathway in *Leishmania* and enable analysis of the sterol profiles of drug-resistant lines, such as amphotericin B resistant *Leishmania* parasites with altered sterol biosynthesis, (Pountain et al., 2019) facilitating discovery of potential surrogate markers for drug susceptibility. However, the method presents two limitations. First, episterol (C_{28} $\Delta^{7,24(28)}$), fecosterol (C_{28} $\Delta^{8,24(28)}$), and 4-methylzymosterol (C_{28} $\Delta^{8,24}$) are indistinguishable by the LC-MRM detection due to having the same molecular weight and similar chemical structure. Second, zymosterol (C_{27} $\Delta^{8,24}$) and cholesta-7,24-dienol (C_{27} $\Delta^{7,24}$) could not be consistently distinguished because they are isomers, and their mass spectra are practically identical. Further optimization of the LC method, such as employing multiple solvent gradient (e.g., methanol/water vs. methanol/acetone/*n*-hexane), may be sufficient to separate isomers differing only in the double bond position (Nagy et al., 2006). Due to lack of synthetic standard, the identification of 14-methylfecosterol and 4,14-dimethylzymosterol (which are isomers of C_{29}-sterol T-MAS), 14-methylzymosterol and ergosta-5,7-dienol (which are isomers of C_{28}-sterol episterol), and 5-dehydrosterolepisterol (which is an isomer of C_{28}-triene sterol ergosterol) was challenging. However, using the structural differences of the sterols (e.g., additional methyl/-methylene groups and/or saturated carbon-carbon bonds), sterols with
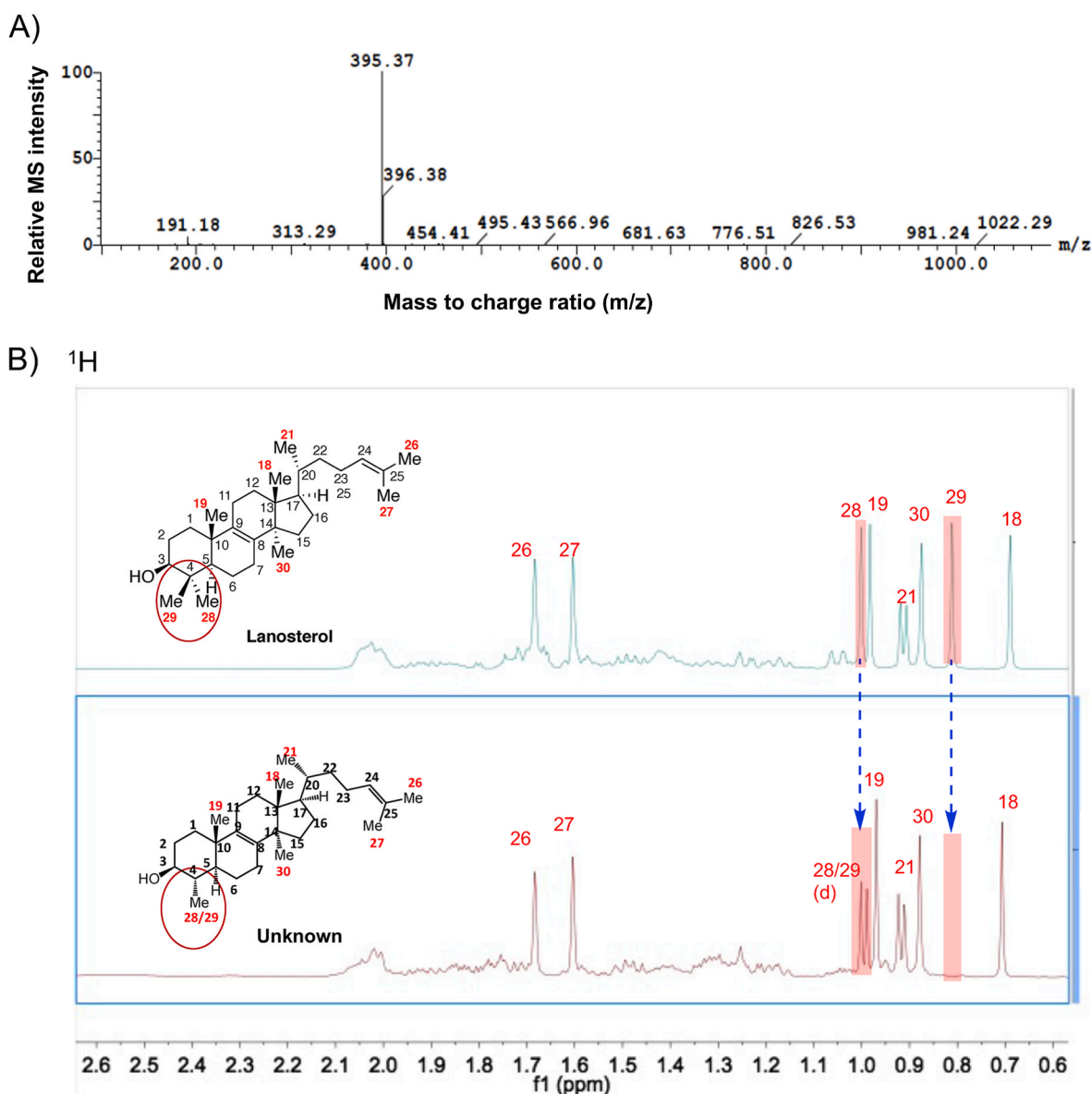
Fig. 5. Structural determination of the purified intermediate sterol 4,14-dimethylzymosterol. (A) The exact mass of the dehydrated precursor ion was determined by high resolution TOF mass spectrometry. (B–G) The 1D and 2D NMR spectra of lanosterol (reference) and the purified intermediate sterol. ^{1}H spectra (B), DEPT (C–E), HMBC (F, G), and NOESY (H, I). 4,14-Dimethylzymosterol is referred to as "unknown" in the figures.

identical masses were identified based on their LC elution order (Table 1) (Armitage et al., 2018).

Previous studies suggested the post-squalene sterol biosynthesis pathway in *Leishmania* species might bifurcate into more than one branch (Beach et al., 1988; Goad and Holz, 1985; Hargrove et al., 2011). The presence of a trace amount of 4,14-dimethylzymosterol indicates that C4-demethylation occurs early in the pathway (Fig. 3 and Scheme 1). Eburicol, obtusifoliol, and 4,4-dimethylfecosterol were not detected in any WT strains examined or antifungal azole-treated promastigotes, indicating that the C24-methylation reactions happen only after C4-demethylation of lanosterol. The detection of episterol and fecosterol suggested the zymosterol C24-methylation happened before C8-isomerization in the pathway (Fig. 3 and Scheme 1). 5-Dehydroepisterol can be formed from addition of a Δ^5 double bond to episterol, catalyzed by Δ^5-desaturase. It appears that the C24-methylation can also happen after C8-isomerization and Δ^5-desaturation of zymosterol, resulting in the formation of cholesta-7,24-dienol,

7-dehydrodesmosterol, and 5-dehydroepisterol. The presence of ergosta-5,7-dienol and ergostatetraenol suggests that the reaction sequences of $\Delta^{24(28)}$-reduction and Δ^{22}-desaturation may vary in their order to form ergosterol. Taken together, our own and previously reported observations support the proposed branched ergosterol biosynthetic pathway as shown in Scheme 1. It should also be noted that there are other un-identified peaks in the LC-MRM chromatograms of sterol extracts of untreated *L. donovani* promastigotes (Fig. 2B) and azole-treated promastigotes (Fig. 2C and D). This suggests that the ergosterol biosynthetic pathway in *Leishmania* could be more complex than what is proposed in Scheme 1, which requires further investigation in the future.

5-Dehydroepisterol has been reported as the most abundant sterol in several *Leishmania* promastigote strains (Goad and Holz, 1984; Gomez-Eichelmann et al., 1988; Haughan et al., 1993). For *L. major* LRC-L38 strain, episterol was identified as the major sterol, which accounted for 42% of the total sterol (Goad and Holz, 1984). In LV39 strain, it's been
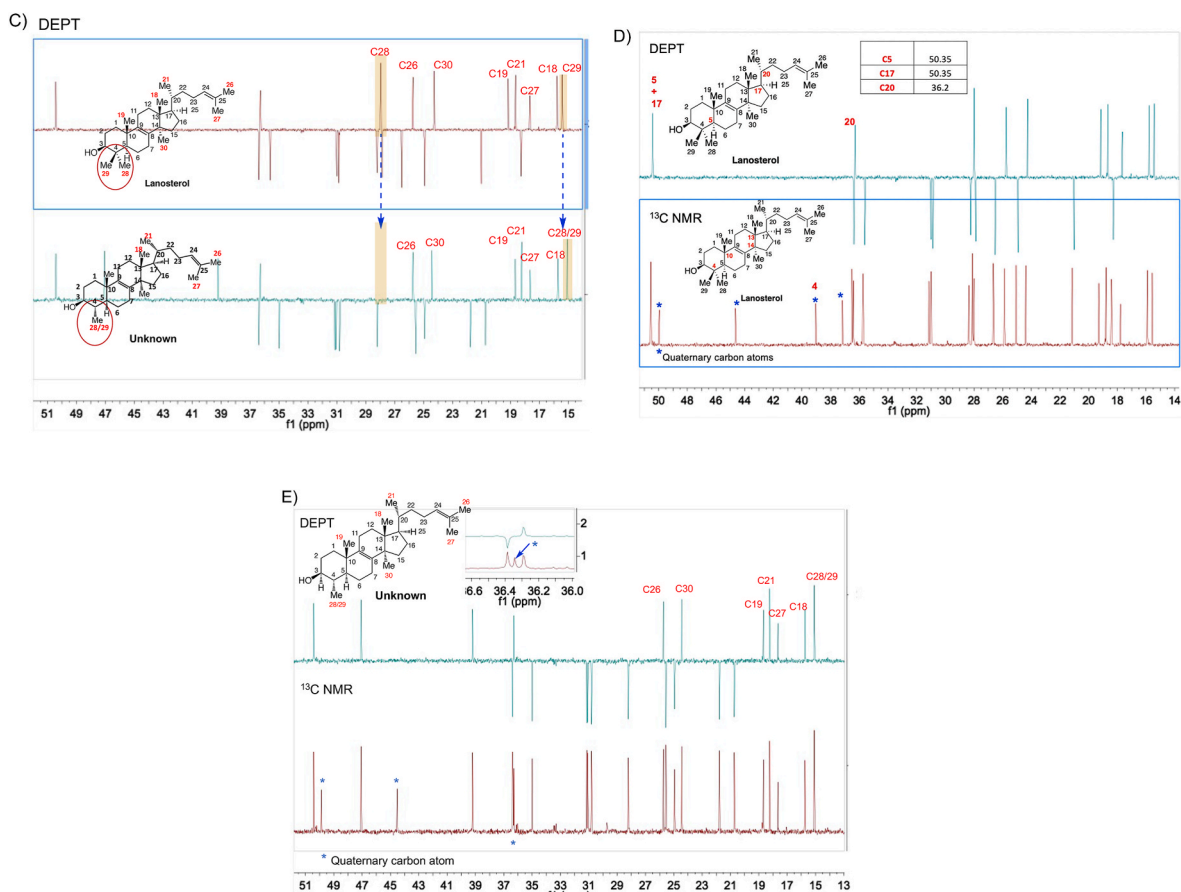
Fig. 5. (*continued*).

observed that ergosterol was the major sterol although significant amounts of 5-dehydroepisterol were also detected (Mukherjee et al., 2019). In our present investigation of the LV39 strain, both 5-dehydroepisterol and ergosterol were readily detected (Fig. 3), although relative concentrations could not be ascertained due to the lack of an authentic standard of 5-dehydroepisterol. Compared to LV39, Ld1s, and LV82, *L. tarentolae* UC strain produced the highest level of ergostatetraenol and the lowest level of ergosterol (Fig. 3), suggesting ergostatetraenol as the major final sterol for the *L. tarentolae* UC strain and that there may be more limited $\Delta^{24(28)}$-reductase activity in the *L. tarentolae* UC promastigotes (Scheme 1).

Antifungal azoles have differential effects on both leishmanial growth and sterol profiles. Consistent with previous studies with *L. donovani* axenic amastigotes (Pandharkar et al., 2014) and with *L. amazonensis* and *L. major* intracellular amastigotes (Buckner and Wilson, 2005), PSZ displayed a much more dramatic effect on *L. donovani* and *L. tarentolae* promastigote growth than FLU (Figs. S3 and S4). When the *L. donovani* promastigote growth inhibition measured by the MTS/PMS assay and by microscopic enumeration (at 5, 10 and 20 μM for PSZ and 12.5, 25 and 50 μM for FLU) were compared, similar trends were observed for PSZ and FLU (data not shown). In addition, the lack of inhibitory activity by FLU was also previously reported for several species of *Leishmania* parasites by microscopic enumeration (IC$_{50}$ values greater than 50 μg/mL) (Kulkarni et al., 2013). These observations indicate a good agreement between tetrazolium-based proliferation assays and direct cell counting for these antifungal azoles, although the risk of test compounds affecting mitochondrial membrane potential and/or metabolism and, consequently, tetrazolium-based proliferation assays should always be assessed for new compounds. To further reveal the differential effects of PSZ and FLU against *L. donovani*, we compared the sterol profiles of PSZ- and FLU-treated promastigotes to the

vehicle-treated control promastigotes. In PSZ-treated LV82, there was a substantial accumulation of lanosterol and 4α,14α-dimethylzymosterol, in contrast to little to moderate accumulation in FLU-treated LV82 (Table 1). In FLU-treated LV82, significant accumulation of C4-desmethyl sterols (14-methylfecosterol and 14-methylzymosterol) and 4α,14α-dimethylzymosterol was observed, in contrast to little accumulation of the C4-desmethyl sterols in PSZ-treated LV82 (Table 1). It appears that PSZ (at 20 μM) inhibited ergosterol biosynthesis at earlier steps: complete inhibition of the lanosterol C14-demethylation reaction and partial inhibition of the lanosterol C4-demethylation reaction, leading to the formation and accumulation of 4α,14α-dimethylzymosterol upon inhibition of subsequent C4 and C14-demethylation reactions (likely by PSZ; Scheme 1 and Table 1). In *L. tarentolae* promastigotes treated with PSZ (at 5 μM), a higher concentration of PSZ was likely needed for more effective inhibition of the 4-demethylation steps, providing a possible explanation for the accumulation of 14-methylzymosterol (Scheme 1 and Table 1). In comparison to PSZ, FLU (at 50 or 100 μM) disrupted ergosterol biosynthesis at different steps, i.e., only C14-demethylation reactions were inhibited whereas C4-demethylation reactions were not affected (Scheme 1 and Table 1). This selective inhibition of C14-demethylation reactions by FLU allowed the conversion of lanosterol to 4,14-dimethylzymosterol by C4-demethylation, resulting in the lack of lanosterol accumulation in FLU-treated *L. donovani* (Table 1). Once again, these observations support the proposed branched ergosterol biosynthetic pathway as shown in Scheme 1.

Considering the branched pathway and the greatly reduced anti-leishmanial potency of fluconazole (likely a selective sterol 14-demethylase [CYP51] inhibitor) relative to posaconazole (likely a dual inhibitor of sterol 4-demethylase and 14-demethylase), we believe that selective inhibition of leishmanial CYP51 is insufficient to effectively prevent parasite growth, and dual inhibitors of both CYP51 and sterol 4-
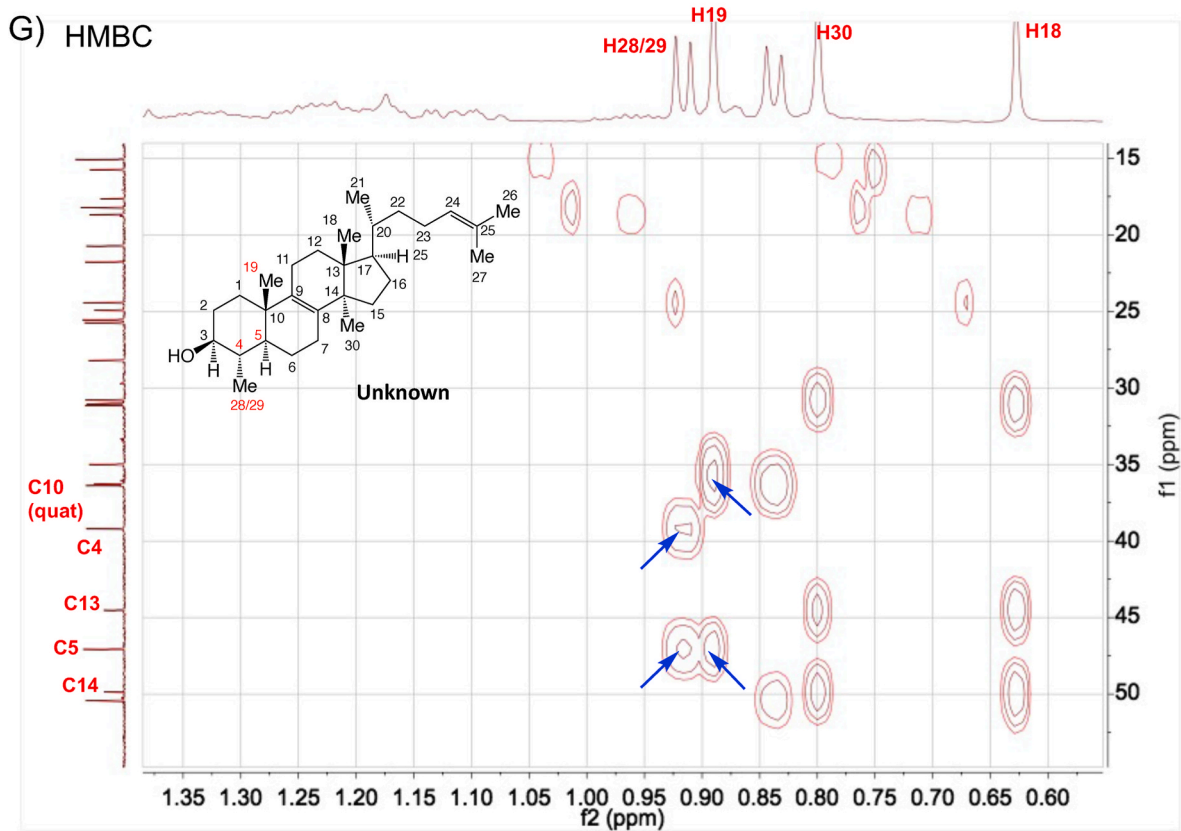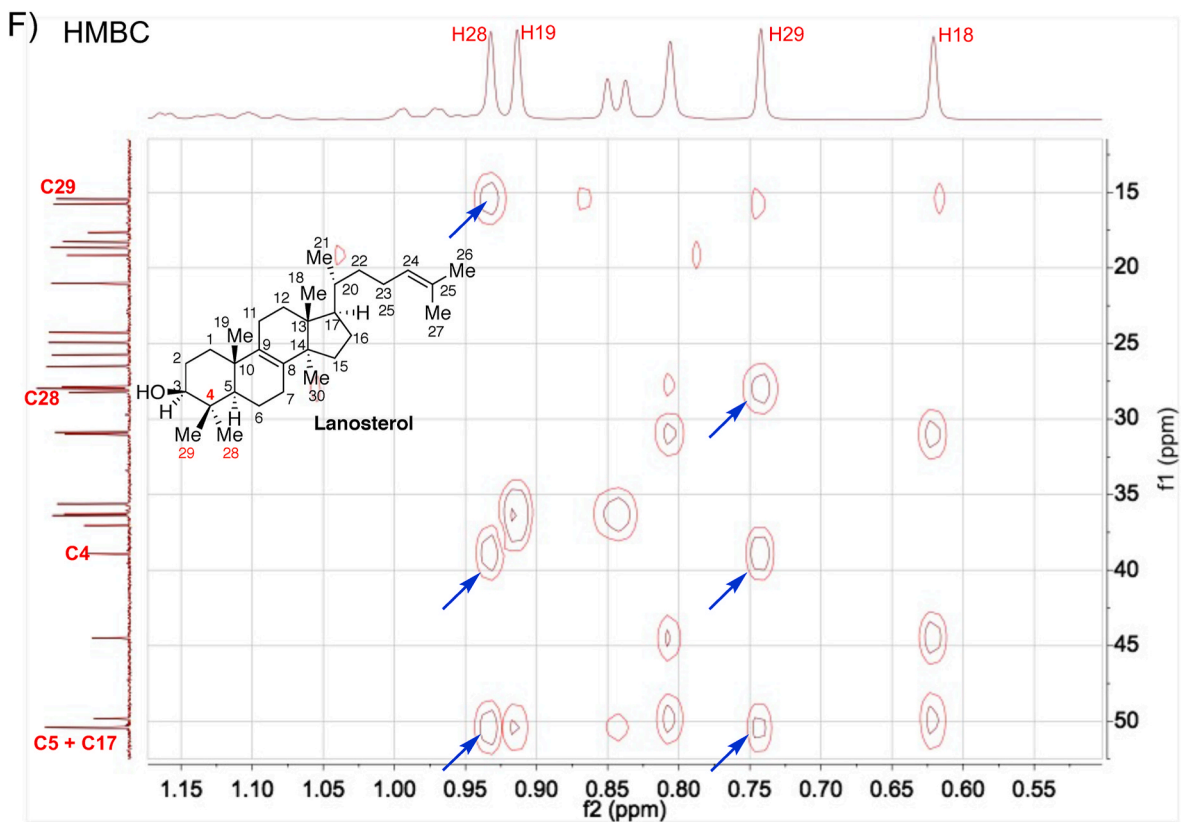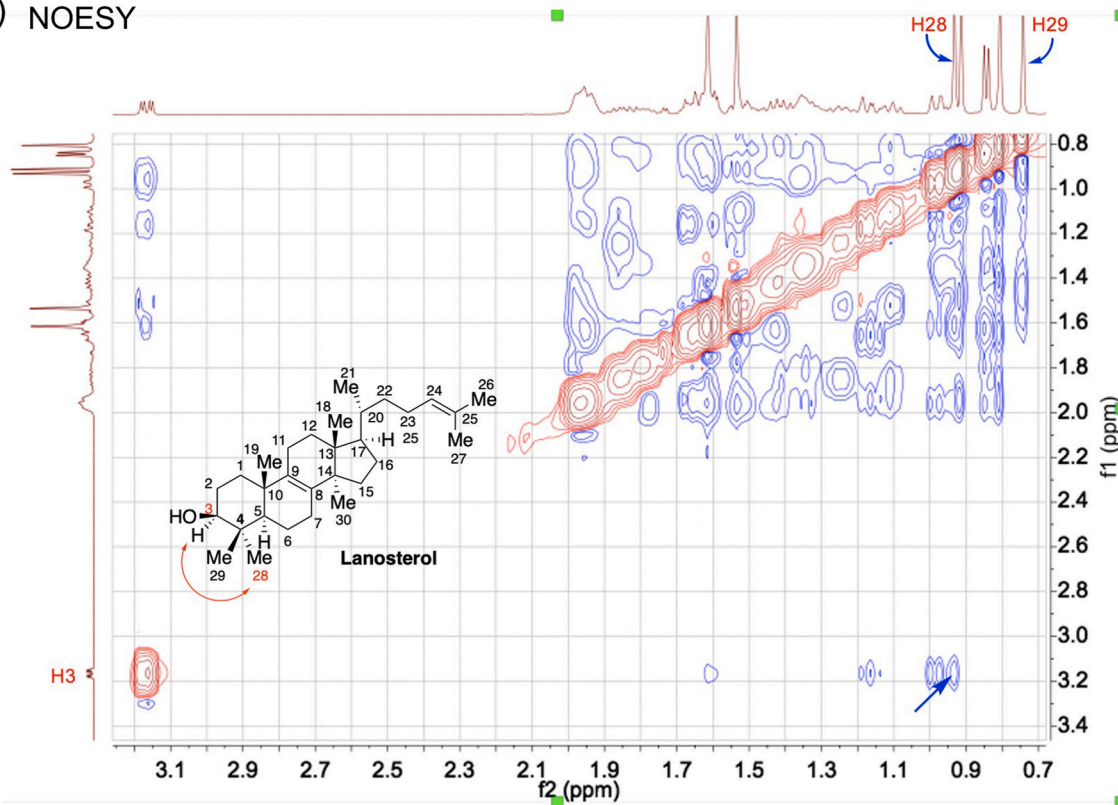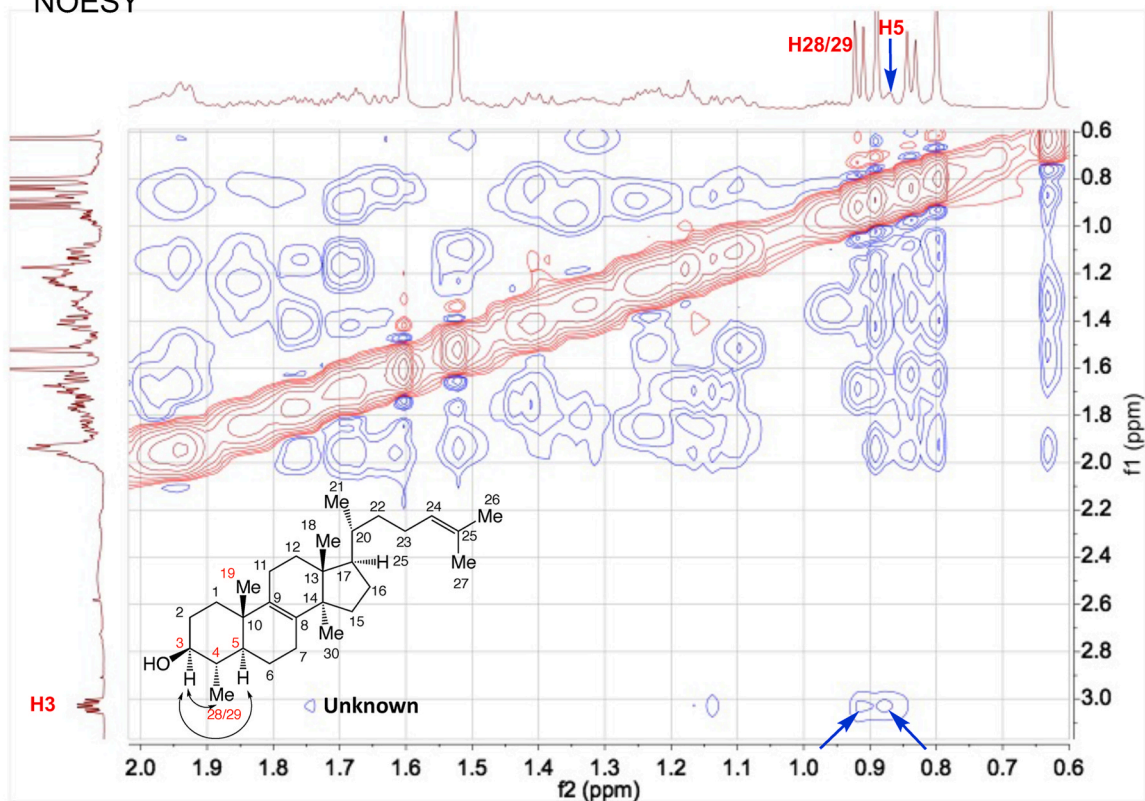
Fig. 5. (*continued*).

Fig. 5. (*continued*).

---

demethylase may be required. 14-Methylfecosterol and 14-methylzymosterol (both are C4-desmethylsterols) appear to be less toxic sterol intermediates compared to methylated sterols like lanosterol, as it was reported that C4-desmethylsterols were able to provide a functional sterol for cell growth by compensating the depletion of ergosterol and/or by stabilizing the membrane against the disruptive effects of lanosterol (Xu et al., 2014; Watson et al., 1989). This may explain why fluconazole was much less toxic to *Leishmania* parasites despite the apparent depletion of ergosterol and ergosterol-like sterols, because it failed to accumulate lanosterol (Table 1). In contrast, posaconazole was able to accumulate lanosterol by inhibiting both 4- and 14-demethylation reactions (Scheme 1). As such, dual inhibitors of both C14-demethylation and C4-demethylation should be more promising antileishmanial drug candidates than selective CYP51 inhibitors. Work is in progress to identify and characterize the novel enzyme responsible for catalyzing the lanosterol C4-demethylation to form the key intermediate sterol 4,14-dimethylzymosterol.

In summary, a key intermediate sterol 4α,14α-dimethylzymosterol was purified and its structural stereochemistry was assigned through 1D and 2D NMR. Our sterol profile analysis using antifungal azoles as chemical probes supported the proposed branched ergosterol biosynthesis pathway in *Leishmania donovani*. Our study and previous reports suggest that selective inhibition of leishmanial CYP51 is insufficient to effectively prevent parasite growth and dual inhibitors of both CYP51 and sterol C4-demethylase may be required.

Funding and competing interest statements

MF currently is an employee of AbbVie and may own AbbVie stock. AbbVie did not participate in any process in the development for this manuscript, and all work was done prior to MF's employment at AbbVie. Authors declare no competing interests.

Financial disclosure

Declaration of competing interest

Authors declare no competing interests or conflict of interest.

Appendix A. Supplementary data

Supplementary data to this article can be found online at https://doi.org/10.1016/j.ijpddr.2022.07.003.

References

Alemayehu, B., Alemayehu, M., 2017. Leishmaniasis: a review on parasite, vector and reservoir host. Health Sci. J. 11 (4) https://doi.org/10.21767/1791-809x.1000519.

Armitage, E.G., Alqaisi, A.Q.I., Godzien, J., Pena, I., Mbekeani, A.J., Alonso-Herranz, V., Lopez-Gonzalvez, A., Martin, J., Gabarro, R., Denny, P.W., Barrett, M.P., Barbas, C., 2018. Complex interplay between sphingolipid and sterol metabolism revealed by perturbations to the leishmania metabolome caused by miltefosine. Antimicrob. Agents Chemother. 62 (5) https://doi.org/10.1128/AAC.02095-17. Epub 20180426 PubMed PMID: 29463533; PMCID: PMC5923112.

Beach, D.H., Holz Jr., G.G., Anekwe, G.E., 1979. Lipids of leishmania promastigotes. J. Parasitol. 65 (2), 201–216. Epub 1979/04/01. PubMed PMID: 448607.

Beach, D.H., Goad, L.J., Holz Jr., G.G., 1988. Effects of antimycotic azoles on growth and sterol biosynthesis of Leishmania promastigotes. Mol. Biochem. Parasitol. 31 (2), 149–162. PubMed PMID: 2847043.

Berman, J.D., Holz Jr., G.G., Beach, D.H., 1984. Effects of ketoconazole on growth and sterol biosynthesis of Leishmania mexicana promastigotes in culture. Mol. Biochem. Parasitol. 12 (1), 1–13. Epub 1984/05/01. PubMed PMID: 6087138.

Buckner, F.S., Wilson, A.J., 2005. Colorimetric assay for screening compounds against Leishmania amastigotes grown in macrophages. Am. J. Trop. Med. Hyg. 72 (5), 600–605. Epub 2005/05/14. doi: 72/5/600 [pii]. PubMed PMID: 15891135.

Calvopina, M., Guevara, A.G., Armijos, R.X., Hashiguchi, Y., Davidson, R.N., Cooper, P. J., 2004. Itraconazole in the treatment of New World mucocutaneous leishmaniasis. Int. J. Dermatol. 43 (9), 659–663. https://doi.org/10.1111/j.1365-4632.2004.02183.x. Epub 2004/09/11 PubMed PMID: 15357745.

Current treatment of leishmaniasis: A Review. doi: 10.2174/1876512100901010009.

Dawit, G., Girma, Z., Simenew, K., 2013. A review on biology, epidemiology and public Health significance of leishmaniasis. J. Bacteriol. Parasitol. 4 (2) https://doi.org/10.4172/2155-9597.1000166.

de Macedo-Silva, S.T., Urbina, J.A., de Souza, W., Rodrigues, J.C., 2013. In vitro activity of the antifungal azoles itraconazole and posaconazole against Leishmania amazonensis. PLoS One 8 (12), e83247. https://doi.org/10.1371/journal.pone.0083247. Epub 20131223 PubMed PMID: 24376670; PMCID: PMC3871555.

de Menezes, J.P., Guedes, C.E., Petersen, A.L., Fraga, D.B., Veras, P.S., 2015. Advances in development of new treatment for leishmaniasis, 2015 BioMed Res. Int., 815023. https://doi.org/10.1155/2015/815023. Epub 2015/06/17 PubMed PMID: 26078965; PMCID: PMC4442256.

de Souza, W., Rodrigues, J.C., 2009. Sterol biosynthesis pathway as target for anti-trypanosomatid drugs, 2009 Interdiscip. Perspect. Infect. Dis., 642502. https://doi.org/10.1155/2009/642502. Epub 2009/08/15 PubMed PMID: 19680554; PMCID: PMC2721973.

Delfin, D.A., Morgan, R.E., Zhu, X., Werbovetz, K.A., 2009. Redox-active dinitrodiphenylthioethers against Leishmania: synthesis, structure-activity relationships and mechanism of action studies. Bioorg. Med. Chem. 17 (2), 820–829. https://doi.org/10.1016/j.bmc.2008.11.031. Epub 2008/12/09 PubMed PMID: 19058972.

Dorlo, T.P.C., Kip, A.E., Younis, B.M., Ellis, S.J., Alves, F., Beijnen, J.H., Njenga, S., Kirigi, G., Hailu, A., Olobo, J., Musa, A.M., Balasegaram, M., Wasunna, M., Karlsson, M.O., Khalil, E.A.G., 2017. Visceral leishmaniasis relapse hazard is linked to reduced miltefosine exposure in patients from Eastern Africa: a population pharmacokinetic/pharmacodynamic study. J. Antimicrob. Chemother. 72 (11), 3131–3140. https://doi.org/10.1093/jac/dkx283. Epub 2017/09/30 PubMed PMID: 28961737; PMCID: PMC5890687.

Emmons, G.T., Wilson, W.K., Schroepfer Jr., G.J., 1989. 24,25-epoxysterols. Differentiation of 24R and 24S epimers by 13C nuclear magnetic resonance spectroscopy. J. Lipid Res. 30 (1), 133–138. Epub 1989/01/01. PubMed PMID: 2918248.

Freitas-Junior, L.H., Chatelain, E., Kim, H.A., Siqueira-Neto, J.L., 2012. Visceral leishmaniasis treatment: what do we have, what do we need and how to deliver it? Int. J. Parasitol. Drugs Drug Resist. 2, 11–19. https://doi.org/10.1016/j.ijpddr.2012.01.003. Epub 2012/12/01 PubMed PMID: 24533267; PMCID: PMC3862432.

Fritsche, C., Sitz, M., Weiland, N., Breitling, R., Pohl, H.D., 2007. Characterization of the growth behavior of Leishmania tarentolae: a new expression system for recombinant proteins. J. Basic Microbiol. 47 (5), 384–393. https://doi.org/10.1002/jobm.200710111. Epub 2007/10/03 PubMed PMID: 17910102.

Ghorbani, M., Farhoudi, R., 2018. Leishmaniasis in humans: drug or vaccine therapy? Drug Des. Dev. Ther. 12, 25–40. https://doi.org/10.2147/DDDT.S146521. Epub 2018/01/11. PubMed PMID: 29317800; PMCID: PMC5743117.

Goad, L.J., Holz Jr., G.G., 1984. Beach DH. Sterols of Leishmania species. Implications for biosynthesis. Mol. Biochem. Parasitol. 10 (2), 161–170. Epub 1984/02/01. PubMed PMID: 6700638.

Goad, L.J., Holz Jr., G.G., 1985. Beach DH. Sterols of ketoconazole-inhibited Leishmania mexicana mexicana promastigotes. Mol. Biochem. Parasitol. 15 (3), 257–279. https://doi.org/10.1016/0166-6851(85)90089-1. Epub 1985/06/01 PubMed PMID: 4033689.

Goad, L.J., 1997. In: Akihisa, T., 秋久俊博 (Eds.), Analysis of Sterols. London : Blackie Academic & Professional, London.

Gomez-Eichelmann, M.C., Holz Jr., G., Beach, D., Simpson, A.M., Simpson, L., 1988. Comparison of several lizard Leishmania species and strains in terms of kinetoplast minicircle and maxicircle DNA sequences, nuclear chromosomes, and membrane lipids. Mol. Biochem. Parasitol. 27 (2–3), 143–158. https://doi.org/10.1016/0166-6851(88)90034-5. Epub 1988/01/15 PubMed PMID: 3344003.

Gray, K.C., Palacios, D.S., Dailey, I., Endo, M.M., Uno, B.E., Wilcock, B.C., Burke, M.D., 2012. Amphotericin primarily kills yeast by simply binding ergosterol. Proc. Natl.

Acad. Sci. U. S. A. 109 (7), 2234–2239. https://doi.org/10.1073/pnas.1117280109. Epub 2012/02/07 PubMed PMID: 22308411; PMCID: PMC3289339.

Griffiths, W.J., Wang, Y., 2009. Analysis of neurosterols by GC-MS and LC-MS/MS. J. Chromatogr., B: Anal. Technol. Biomed. Life Sci. 877 (26), 2778–2805. https://doi.org/10.1016/j.jchromb.2009.05.017. Epub 2009/06/30 PubMed PMID: 19560986.

Hailu, A., Musa, A., Wasunna, M., Balasegaram, M., Yifru, S., Mengistu, G., Hurissa, Z., Hailu, W., Weldegebreal, T., Tesfaye, S., Makonnen, E., Khalil, E., Ahmed, O., Fadlalla, A., El-Hassan, A., Raheem, M., Mueller, M., Koummuki, Y., Rashid, J., Mbui, J., Mucee, G., Njoroge, S., Manduku, V., Musibi, A., Mutuma, G., Kirui, F., Lodenyo, H., Mutea, D., Kirigi, G., Edwards, T., Smith, P., Muthami, L., Royce, C., Ellis, S., Alobo, M., Omollo, R., Kesusu, J., Owiti, R., Kinuthia, J., 2010. Leishmaniasis East Africa Platform g. Geographical variation in the response of visceral leishmaniasis to paromomycin in East Africa: a multicentre, open-label, randomized trial. PLoS Neglected Trop. Dis. 4 (10), e709. https://doi.org/10.1371/journal.pntd.0000709. Epub 20101026. PubMed PMID: 21049059; PMCID: PMC2964287.

Hargrove, T.Y., Wawrzak, Z., Liu, J., Nes, W.D., Waterman, M.R., Lepesheva, G.I., 2011. Substrate preferences and catalytic parameters determined by structural characteristics of sterol 14alpha-demethylase (CYP51) from Leishmania infantum. J. Biol. Chem. 286 (30), 26838–26848. https://doi.org/10.1074/jbc.M111.237099. PubMed PMID: 21632531; PMCID: PMC3143644.

Haughan, P.A., Chance, M.L., Goad, L.J., 1993. Effects of sinefungin on growth and sterol composition of Leishmania promastigotes. Exp. Parasitol. 77 (2), 147–154. https://doi.org/10.1006/expr.1993.1071. Epub 1993/09/01 PubMed PMID: 8375483.

Igarashi, F., Hikiba, J., Ogihara, M.H., Nakaoka, T., Suzuki, M., Kataoka, H., 2011. A highly specific and sensitive quantification analysis of the sterols in silkworm larvae by high performance liquid chromatography-atmospheric pressure chemical ionization-tandem mass spectrometry. Anal. Biochem. 419 (2), 123–132. https://doi.org/10.1016/j.ab.2011.08.046. Epub 2011/09/20 PubMed PMID: 21925474.

Joice, A.C., Yang, S., Farahat, A.A., Meeds, H., Feng, M., Li, J., Boykin, D.W., Wang, M.Z., Werbovetz, K.A., 2018. Antileishmanial efficacy and pharmacokinetics of DB766-azole combinations. Antimicrob. Agents Chemother. 62 (1) https://doi.org/10.1128/AAC.01129-17. Epub 20171221 PubMed PMID: 29061761; PMCID: PMC5740383.

Kapler, G.M., Coburn, C.M., Beverley, S.M., 1990. Stable transfection of the human parasite Leishmania major delineates a 30-kilobase region sufficient for extrachromosomal replication and expression. Mol. Cell Biol. 10 (3), 1084–1094. https://doi.org/10.1128/mcb.10.3.1084. Epub 1990/03/01 PubMed PMID: 2304458; PMCID: PMC360971.

Kulkarni, M.M., Reddy, N., Gude, T., McGwire, B.S., 2013. Voriconazole suppresses the growth of Leishmania species in vitro. Parasitol. Res. 112 (5), 2095–2099. https://doi.org/10.1007/s00436-013-3274-x. Epub 2013/02/09 PubMed PMID: 23392902.

Kumar, R., Pandey, K., Sahoo, G.C., Das, S., Das, V., Topno, R.K., Das, P., 2017. Development of high efficacy peptide coated iron oxide nanoparticles encapsulated amphotericin B drug delivery system against visceral leishmaniasis. Mater. Sci. Eng. C Mater. Biol. Appl. 75, 1465–1471. https://doi.org/10.1016/j.msec.2017.02.145. Epub 2017/04/19 PubMed PMID: 28415438.

Maarouf, M., de Kouchkovsky, Y., Brown, S., Petit, P.X., Robert-Gero, M., 1997. In vivo interference of paromomycin with mitochondrial activity of Leishmania. Exp. Cell Res. 232 (2), 339–348. https://doi.org/10.1006/excr.1997.3500. Epub 1997/05/01 PubMed PMID: 9168801.

Magaraci, F., Jimenez, C.J., Rodrigues, C., Rodrigues, J.C., Braga, M.V., Yardley, V., de Luca-Fradley, K., Croft, S.L., de Souza, W., Ruiz-Perez, L.M., Urbina, J., Gonzalez Pacanowska, D., Gilbert, I.H., 2003. Azasterols as inhibitors of sterol 24-methyl-transferase in Leishmania species and Trypanosoma cruzi. J. Med. Chem. 46 (22), 4714–4727. https://doi.org/10.1021/jm021114j. Epub 2003/10/17 PubMed PMID: 14561091.

McCall, L.I., El Aroussi, A., Choi, J.Y., Vieira, D.F., De Muylder, G., Johnston, J.B., Chen, S., Kellar, D., Siqueira-Neto, J.L., Roush, W.R., Podust, L.M., McKerrow, J.H., 2015. Targeting Ergosterol biosynthesis in Leishmania donovani: essentiality of sterol 14 alpha-demethylase. PLoS Neglected Trop. Dis. 9 (3), e0003588 https://doi.org/10.1371/journal.pntd.0003588. PubMed PMID: 25768284; PMCID: PMC4359151.

Millerioux, Y., Mazet, M., Bouyssou, G., Allmann, S., Kiema, T.R., Bertiaux, E., Fouillen, L., Thapa, C., Biran, M., Plazolles, N., Dittrich-Domergue, F., Crouzols, A., Wierenga, R.K., Rotureau, B., Moreau, P., Bringaud, F., 2018. De novo biosynthesis of sterols and fatty acids in the Trypanosoma brucei procyclic form: carbon source preferences and metabolic flux redistributions. PLoS Pathog. 14 (5), e1007116 https://doi.org/10.1371/journal.ppat.1007116. Epub 2018/05/31 PubMed PMID: 29813135; PMCID: PMC5993337.

Mukherjee, S., Xu, W., Hsu, F.F., Patel, J., Huang, J., Zhang, K., 2019. Sterol methyltransferase is required for optimal mitochondrial function and virulence in Leishmania major. Mol. Microbiol. 111 (1), 65–81. https://doi.org/10.1111/mmi.14139. Epub 2018/09/28 PubMed PMID: 30260041; PMCID: PMC6351164.

Nagle, A.S., Khare, S., Kumar, A.B., Supek, F., Buchynskyy, A., Mathison, C.J., Chennamaneni, N.K., Pendem, N., Buckner, F.S., Gelb, M.H., Molteni, V., 2014. Recent developments in drug discovery for leishmaniasis and human African trypanosomiasis. Chem. Rev. 114 (22), 11305–11347. https://doi.org/10.1021/cr500365f. Epub 2014/11/05 PubMed PMID: 25365529; PMCID: PMC4633805.

Nagy, K., Jakab, A., Pollreisz, F., Bongiorno, D., Ceraulo, L., Averna, M.R., Noto, D., Vekey, K., 2006. Analysis of sterols by high-performance liquid chromatography/mass spectrometry combined with chemometrics. Rapid Commun. Mass Spectrom. : RCM (Rapid Commun. Mass Spectrom.) 20 (16), 2433–2440. https://doi.org/10.1002/rcm.2606. Epub 2006/07/15 PubMed PMID: 16841361.

Oliveira, A.L., Brustoloni, Y.M., Fernandes, T.D., Dorval, M.E., Cunha, R.V., Boia, M.N., 2009. Severe adverse reactions to meglumine antimoniate in the treatment of visceral leishmaniasis: a report of 13 cases in the southwestern region of Brazil. Trop. Doct. 39 (3), 180–182. https://doi.org/10.1258/td.2008.080369. Epub 2009/06/19. PubMed PMID: 19535762.

Oryan, A., Akbari, M., 2016. Worldwide risk factors in leishmaniasis. Asian Pac. J. Trop. Med. 9 (10), 925–932. https://doi.org/10.1016/j.apjtm.2016.06.021. Epub 2016/10/31. PubMed PMID: 27794384.

Palatnik-de-Sousa, C.B., Nico, D., 2020. The delay in the licensing of Protozoal vaccines: a comparative history. Front. Immunol. 11, 204. https://doi.org/10.3389/fimmu.2020.00204. Epub 2020/03/27. PubMed PMID: 32210953; PMCID: PMC7068796.

Pandharkar, T., Zhu, X., Mathur, R., Jiang, J., Schmittgen, T.D., Shaha, C., Werbovetz, K. A., 2014. Studies on the antileishmanial mechanism of action of the arylimidamide DB766: azole interactions and role of CYP5122A1. Antimicrob. Agents Chemother. 58 (8), 4682–4689. https://doi.org/10.1128/AAC.02405-14. Epub 2014/06/04 PubMed PMID: 24890590; PMCID: PMC4135980.

Pountain, A.W., Weidt, S.K., Regnault, C., Bates, P.A., Donachie, A.M., Dickens, N.J., Barrett, M.P., 2019. Genomic instability at the locus of sterol C24-methyltransferase promotes amphotericin B resistance in Leishmania parasites. PLoS Neglected Trop. Dis. 13 (2), e0007052 https://doi.org/10.1371/journal.pntd.0007052. Epub 20190204 PubMed PMID: 30716073; PMCID: PMC6375703.

Raederstorff, D., Rohmer, M., 1986. Sterol biosynthesis via lanosterol by the trypanosomidCrithidia fasciculata. FEMS (Fed. Eur. Microbiol. Soc.) Microbiol. Lett. 34 (3), 269–272. https://doi.org/10.1111/j.1574-6968.1986.tb01418.x.

Raymond, F., Boisvert, S., Roy, G., Ritt, J.F., Legare, D., Isnard, A., Stanke, M., Olivier, M., Tremblay, M.J., Papadopoulou, B., Ouellette, M., Corbeil, J., 2012. Genome sequencing of the lizard parasite Leishmania tarentolae reveals loss of genes associated with the intracellular stage of human pathogenic species. Nucleic Acids Res. 40 (3), 1131–1147. https://doi.org/10.1093/nar/gkr834. Epub 2011/10/15 PubMed PMID: 21998295; PMCID: PMC3273817.

Razzazi-Fazeli, E., Kleineisen, S., Luf, W., 2000. Determination of cholesterol oxides in processed food using high-performance liquid chromatography-mass spectrometry with atmospheric pressure chemical ionisation. J. Chromatogr., A 896 (1–2), 321–334. https://doi.org/10.1016/s0021-9673(00)00719-6. Epub 2000/11/28 PubMed PMID: 11093667.

Rossmann, B., Thurner, K., Luf, W., 2007. MS-MS fragmentation patterns of cholesterol oxidation products. Monatsh. Chem. 138 (5), 436–444. https://doi.org/10.1007/s00706-007-0589-2. PubMed PMID: WOS:000246276000004.

Seifert, K., 2011. Structures, targets and recent approaches in anti-leishmanial drug discovery and development. Open Med. Chem. J. 5, 31–39. https://doi.org/10.2174/1874104501105010031. Epub 2011/06/02. PubMed PMID: 21629509; PMCID: PMC3103891.

Skubic, C., Vovk, I., Rozman, D., Krizman, M., 2020. Simplified LC-MS method for analysis of sterols in biological samples. Molecules 25 (18). https://doi.org/10.3390/molecules25184116. Epub 2020/09/13 PubMed PMID: 32916848; PMCID: PMC7571030.

Sousa, A.Q., Frutuoso, M.S., Moraes, E.A., Pearson, R.D., Pompeu, M.M., 2011. High-dose oral fluconazole therapy effective for cutaneous leishmaniasis due to Leishmania (Vianna) braziliensis. Clin. Infect. Dis. 53 (7), 693–695. https://doi.org/10.1093/cid/cir496. Epub 2011/09/06 PubMed PMID: 21890773.

Sundar, S., 2001. Drug resistance in Indian visceral leishmaniasis. Trop. Med. Int. Health 6 (11), 849–854. https://doi.org/10.1046/j.1365-3156.2001.00778.x. Epub 2001/11/13. PubMed PMID: 11703838.

Sundar, S., Jha, T.K., Thakur, C.P., Sinha, P.K., Bhattacharya, S.K., 2007. Injectable paromomycin for Visceral leishmaniasis in India. N. Engl. J. Med. 356 (25), 2571–2581. https://doi.org/10.1056/NEJMoa066536. Epub 2007/06/22. PubMed PMID: 17582067.

Teixeira de Macedo Silva, S., Visbal, G., Lima Prado Godinho, J., Urbina, J.A., de Souza, w., Cola Fernandes Rodrigues, J., 2018. In vitro antileishmanial activity of ravuconazole, a triazole antifungal drug, as a potential treatment for leishmaniasis. J. Antimicrob. Chemother. 73 (9), 2360–2373. https://doi.org/10.1093/jac/dky229. Epub 2018/07/10 PubMed PMID: 29982734.

Torres-Guerrero, E., Quintanilla-Cedillo, M.R., Ruiz-Esmenjaud, J., 2017. Arenas R. Leishmaniasis: a review. F1000Res 6, 750. https://doi.org/10.12688/f1000research.11120.1. Epub 2017/06/27. PubMed PMID: 28649370; PMCID: PMC5464238.

Trosken, E.R., Straube, E., Lutz, W.K., Volkel, W., Patten, C., 2004. Quantitation of lanosterol and its major metabolite FF-MAS in an inhibition assay of CYP51 by azoles with atmospheric pressure photoionization based LC-MS/MS. J. Am. Soc. Mass Spectrom. 15 (8), 1216–1221. https://doi.org/10.1016/j.jasms.2004.04.036. Epub 2004/07/28 PubMed PMID: 15276168.

Trosken, E.R., Adamska, M., Arand, M., Zarn, J.A., Patten, C., Volkel, W., Lutz, W.K., 2006. Comparison of lanosterol-14 alpha-demethylase (CYP51) of human and Candida albicans for inhibition by different antifungal azoles. Toxicology 228 (1), 24–32. https://doi.org/10.1016/j.tox.2006.08.007. PubMed PMID: 16989930.

Urbina, J.A., Concepcion, J.L., Rangel, S., Visbal, G., Lira, R., 2002. Squalene synthase as a chemotherapeutic target in Trypanosoma cruzi and Leishmania mexicana. Mol. Biochem. Parasitol. 125 (1–2), 35–45. https://doi.org/10.1016/s0166-6851(02)00206-2. Epub 2002/12/07 PubMed PMID: 12467972.

Wali, J.P., Aggarwal, P., Gupta, U., Saluja, S., Singh, S., 1990. Ketoconazole in treatment of visceral leishmaniasis. Lancet 336 (8718), 810–811. https://doi.org/10.1016/0140-6736(90)93272-q. Epub 1990/09/29 PubMed PMID: 1976166.

Watson, P.F., Rose, M.E., Ellis, S.W., England, H., Kelly, S.L., 1989. Defective sterol C5-6 desaturation and azole resistance: a new hypothesis for the mode of action of azole

antifungals. Biochem. Biophys. Res. Commun. 164 (3), 1170–1175. https://doi.org/10.1016/0006-291x(89)91792-0. Epub 1989/11/15 PubMed PMID: 2556119.

Wise, E.S., Armstrong, M.S., Watson, J., Lockwood, D.N., 2012. Monitoring toxicity associated with parenteral sodium stibogluconate in the day-case management of returned travellers with New World cutaneous leishmaniasis [corrected]. PLoS Neglected Trop. Dis. 6 (6), e1688. https://doi.org/10.1371/journal.pntd.0001688. Epub 2012/06/30. PubMed PMID: 22745840; PMCID: PMC3383730.

World Health Organization. Epidemiological situation 2020. Available from: https://www.who.int/leishmaniasis/burden/en/.

Xu, W., Hsu, F.F., Baykal, E., Huang, J., Zhang, K., 2014. Sterol biosynthesis is required for heat resistance but not extracellular survival in leishmania. PLoS Pathog. 10 (10), e1004427 https://doi.org/10.1371/journal.ppat.1004427. Epub 20141023 PubMed PMID: 25340392; PMCID: PMC4207814.

Yakovich, A.J., Ragone, F.L., Alfonzo, J.D., Sackett, D.L., Werbovetz, K.A., 2006. Leishmania tarentolae: purification and characterization of tubulin and its suitability for antileishmanial drug screening. Exp. Parasitol. 114 (4), 289–296. https://doi.org/10.1016/j.exppara.2006.04.008. Epub 2006/06/07 PubMed PMID: 16753146; PMCID: 1986769.

Yao, C., Wilson, M.E., 2016. Dynamics of sterol synthesis during development of Leishmania spp. parasites to their virulent form. Parasites Vectors 9, 200. https://doi.org/10.1186/s13071-016-1470-0. Epub 20160412 PubMed PMID: 27071464; PMCID: PMC4830053.

Zhang, R., Brennan, M.L., Shen, Z., MacPherson, J.C., Schmitt, D., Molenda, C.E., Hazen, S.L., 2002. Myeloperoxidase functions as a major enzymatic catalyst for initiation of lipid peroxidation at sites of inflammation. J. Biol. Chem. 277 (48), 46116–46122. https://doi.org/10.1074/jbc.M209124200. PubMed PMID: 12359714.

Zulfiqar, B., Shelper, T.B., Avery, V.M., 2017. Leishmaniasis drug discovery: recent progress and challenges in assay development. Drug Discov. Today 22 (10), 1516–1531. https://doi.org/10.1016/j.drudis.2017.06.004. Epub 2017/06/26. PubMed PMID: 28647378.